Fall 1-31-2009

# Dual parametric sensors for highly sensitive nucleic acid detection

Manu Sebastian Mannoor
*New Jersey Institute of Technology*

## ABSTRACT

## DUAL PARAMETRIC SENSORS FOR HIGHLY SENSITIVE NUCLEIC ACID DETECTION

**by**
**Manu Sebastian Mannoor**

The primary focus of this research work was on the design and development of a molecular scale (nano-scale) capacitive sensing mechanism for the highly sensitive and label-free detection of Nucleic Acid hybridization. These novel capacitive sensors with nano-scale electrode spacing offer solutions to many problems suffered by the conventional signal transduction mechanisms, thereby immensely improving the sensitivity of the biomolecular detection processes. Reducing the separation between the capacitive electrodes to the same scale as the Debye length of the sample solution, results in the overlapping of the electrical double layers of the two electrodes, thereby confining them to occupy a major fraction of the dielectric volume. This decreases the potential drop across the electrodes and thus dielectric measurements at low frequencies are made possible. The dielectric properties during hybridization reaction were measured using 10-mer nucleotide sequences. A 30-40% change in relative permittivity (capacitance) was observed due to DNA hybridization at 10Hz, which is much more sensitive than the previously reposted detection measurements (2-8% signal change).

In parallel to the above work, a second label-free sensing mechanism based on field effect capacitive sensors with Metal-Oxide-Semiconductor (MOS) structure has been developed and its ability to provide real-time monitoring of oligonucleotide immobilization and hybridization events are studied. The immobilization of probe

oligomers on the sensor surface and their hybridization with the target oligomers of complimentary sequences has produced significant shifts (140mV and 73mV respectively) in the Capacitance-Voltage characteristics measured across the device. In an attempt to utilize the individual merits of the nano-scale electrochemical capacitive sensor and the field effect MOS capacitive structure, a novel dual parametric sensing architecture comprising of both these transducing elements on a single sensor is designed. The detection scheme based on the combined analysis of the two parameters- Dielectric property and intrinsic molecular charge- of Nucleic acid molecules has found to reveal complimentary information of significance about the analyte-probe interactions.

As a separate experiment the applications and promises of a novel technique of enhancing the speed and selectivity of the molecular detection processes by the application of an external electric field of precisely controlled intensity was studied. Experiments were conducted with 10-mer sequences and proved the feasibility of this technique in inducing in providing a faster and selective immobilization and hybridization reactions. The research work in this direction has been in collaboration with the Rational Affinity Devices, LLC, a New Jersey based corporation. The above mentioned biosensing mechanisms and detection techniques have the advantage of simplifying the readout and increasing the speed and ease of nucleic acid assays, which is especially desirable for characterizing infectious agents, scoring sequence polymorphism and genotypes, and measuring mRNA or miRNA levels during expression profiling. Once fully optimized and well assembled they have great potential to be developed in to a commercial full-scale biosensor capable of providing high-value diagnostic testing at the point of patient care places.

# DUAL PARAMETRIC SENSORS FOR HIGHLY SENSITIVE NUCLEIC ACID DETECTION

by
Manu Sebastian Mannoor

A Thesis
Submitted to the Faculty of
New Jersey Institute of Technology
in Partial Fulfillment of the Requirements for the Degree of
Master of Science in Biomedical Engineering

Department of Biomedical Engineering

January 2009

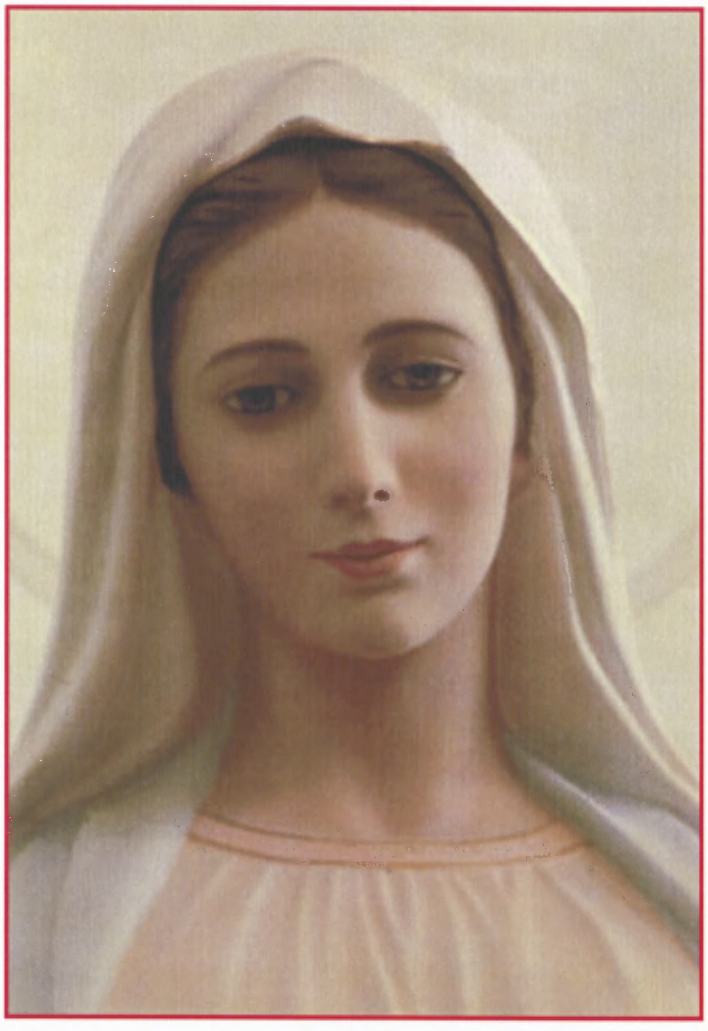

*Dedicated to my Beloved Blessed Mother*

**APPROVAL PAGE**

**DUAL PARAMETRIC SENSORS FOR HIGHLY SENSITIVE NUCLEIC ACID DETCTION**

**Manu Sebastian Mannoor**

11/25/08

Dr. Dentcho V. Ivanov, Thesis Advisor — Date
Director, Microelectronics Fabrication Center, NJIT
Research Professor of Biomedical Engineering, NJIT

11/25/08

Dr. William C. Hunter, Committee Member — Date
Professor of Biomedical Engineering, NJIT

11/25/08

Dr. Treena Arinzeh, Committee Member — Date
Associate Professor of Biomedical Engineering, NJIT

## BIOGRAPHICAL SKETCH

**Author:** Manu Sebastian Mannoor

**Degree:** Master of Science

**Date:** January 2009

**Undergraduate and Graduate Education:**

- Master of Science in Biomedical Engineering,
  New Jersey Institute of Technology, Newark, NJ, 2009

- Bachelor of Science in Electronics & Communication Engineering,
  Government Engineering College, Thrissur, Kerala, India, 2006

**Major:** Biomedical Engineering

**Presentation and Publications:**

1. Manu Sebastian Mannoor, Teena James, Dentcho V. Ivanov, Les Beadling and Bill Braunlin "Debye Capacitive sensor for biomolecular detection" in NSTI Nanotech, Boston, MA, June 20008. (Poster presentation)

2. Manu Sebastian Mannoor, Teena James, Dentcho. V Ivanov, Les Beadling and Bill Braunlin "NEMS Capacitive Sensors for Highly Sensitive Label -Free Nucleic-acid Analysis" Springer-Verlag Lecture Notes of the Institute for Computer Sciences, Social-Informatics and Telecommunications Engineering, 3rd International Conference on Nano-Networks, Boston, MA Sept. 2008. (Oral presentation)

3. Manu Sebastian Mannoor, Teena James, Dentcho. V Ivanov "Active MOS Capacitive Sensor Array for Lab-On-a-Chip Applications" 35th annual conference of Federation of Analytical Chemistry & Spectroscopy Societies (FACSS), Reno, NV, Sept. 2008. (Oral presentation)

4. Manu Sebastian Mannoor, Teena James, Dentcho. V Ivanov, Les Beadling and Bill Braunlin " Ultra Sensitive Debye Capacitive Sensors with Nano-scale Electrode spacing for Label-free Nucleic Acid Analysis " 5th International Congress of Nano-Bio Clean Tech, San Francisco, CA, Oct. 2008. (Oral presentation)

5. Manu Sebastian Mannoor, Teena James, Dentcho. V Ivanov, Les Beadling and Bill Braunlin "Nano-scaled Debye Capacitive Sensors for Highly Sensitive, Label-free, Nucleic Acid Analysis" Materials Research Society (MRS) Fall meeting, Boston, MA, Dec. 2008. (Poster presentation)

6. Teena James, Manu Sebastian Mannoor, Dentcho. V Ivanov, Les Beadling and Bill Braunlin, "Active Field Effect Capacitive Sensor Array for High-Throughput Biomolecular Screening" Materials Research Society (MRS) Fall meeting, Boston, MA, Dec. 2008. (Poster presentation)

7. William Braunlin, Les Beadling, Manu Sebastian Mannoor and Teena James, Tunable Affinity Ligands for the Separation of Proteins and Biomacromolecular Complexes, Biophys. J. 2008 94. (Poster presentation)

8. Manu Sebastian Mannoor, Teena James, Dentcho. V Ivanov, Les Beadling and Bill Braunlin "Label-free affinity based geno-sensors for point-of-care diagnostic applications" SPIE symposium on MOEMS-MEMS, San Jose, CA, Jan. 2009. (Oral presentation)

9. Les Beadling, Manu Sebastian Mannoor, Teena James and William Braunlin,"Tunable Affinity Ligands: A new approach to Affinity Chromatography" Biomaterials in Medicine and Personal Care, New Brunswick, NJ, May 2008.

10. Manu S. Mannoor, Teena James, Dentcho. V Ivanov, "BioMEMS- Advancing the Frontiers of Medicine" Sensors, vol 8, no.9, pp 6077-6177, 2008.

**Book Chapter**

1. Manu Sebastian Mannoor, Teena James and Dentcho V. Ivanov "BioMEMS - Integrating Micro/Nano fabrication with Biomolecular Technologies" in Standard Hand Book of Biomedical Engineering & Design. Myer Kutz (Editor), McGraw-Hill (2008 in press)

**Invited Speeches**

1. NanoTX'08 - International Nanotechnology Conference and Trade Expo, Oct 2-3, 2008, Dallas, Texas. Session: Electronics & Materials.

2. NASA Tech Briefs - National Nano Engineering Conference, (NNEC) Nov 12-13, 2008, Boston, Massachusetts. Session: Diagnostics/Biosensors.

**Invention Disclosures and Patents**

1. Active Dual Parametric Capacitive Biosensors, US Provisional Patent application filed, August, 2008.

## ACKNOWLEDGMENT

I would like to express my sincere gratitude to my advisor, Dr. Dentcho V. Ivanov for his valuable support and guidance throughout the course of my thesis work. My special thanks to Dr. Les Beadling, Dr. Bill Braunlin and Dr. Roger Cubicciotti of Rational Affinity Devices LLC for the inspirational ideas, valuable comments and support without which this work would not have been possible.

I thank the members of my thesis defense committee, Dr. William C. Hunter and Dr. Treena Arinzeh for setting aside their time for me and also for their valuable suggestions and comments. I extend my sincere thanks to Dr. Rajendra Jarwal, process engineer at the Microelectronics Research Center for his valuable suggestions and help during the Micro fabrication procedures. I would also like to thank Dr. Camelia Prodan, Assistant Professor, Department of Physics, for her help with the dielectric spectroscopic measurements. I thank Dr. Durgamadhab Misra, Professor, Department of Electrical and Computer Engineering for allowing me to use his lab and the probe station for measuring the Capacitance –Voltage characteristics.

Finally, I thank my dear Lord, for guiding me in every step of my journey.

## TABLE OF CONTENTS

**TABLE OF CONTENTS**
**(Continued)**

**Chapter** **Page**

## LIST OF FIGURES

## LIST OF FIGURES
## (Continued)

**Figure** **Page**

# CHAPTER 1

# INTRODUCTION

## 1.1 Motivation and Overview

The completion of the human genome project and the advances in the genetic sequencing of pathogenic species have widely encouraged scientists in the development of sensors for Nucleic Acid (DNA or RNA) based diagnostics, pharmaceutical applications, forensic medicine and biowarfare. For instance, an increasingly large number of infectious diseases are diagnosable by the molecular analysis of nucleic acids [1]. Although a number of detection mechanisms utilizing several physiochemical signal transducing principles have been demonstrated over the years, the development of reliable methods for the fast, inexpensive and sensitive detection of nucleic acid sequences is still in its infancy [2-5].

In order to better understand the operating principle of such sensing devices a primary knowledge about the properties of a Nucleic Acid molecules is required. For example a DNA molecule consists of a number of nucleotides which are stacked atop each other in two strands forming a twisted ladder. Each of these nucleotides contain a sugar and phosphate back bone plus one of four molecules called bases-adenine, guanine, cytosine, or thymine (A, T, G, C). These bases form the rugs of the ladder with adenine always across from thymine and guanine always across from cytosine. DNA in its ds state is stable under physiochemical conditions; however strand separation (denaturation) can be achieved by heating above melting temperature, by raising the pH or by lowering the salt concentration [6]. Conversely under appropriate conditions single strands of NA will, provided they are exactly or nearly complimentary in sequence, come together and

"hybridize" to form a duplex molecule via base pairing (adenine pairs with thymine and cytosine with guanine; in the case of DNA-RNA or RNA-RNA duplexes adenine pairs with uracil, U)

Most of the nucleic acid detection techniques are based on a the NA-hybridization reaction where a specific single stranded NA sequence (target) is identified and detected using complimentary sequences called probes [7]. The hybridization reaction is known to be highly efficient and extremely specific in the presence of a mixture of non complimentary sequences and hence can be use as analytical tool to search for and detect the presence of specific sequences in a sample of unknown sequences. For example, for applications such as infectious disease diagnosis hybridization reaction can be used to detect the presence of particular pathogenic sequences in a clinical specimen (eg: throat swab). The key issue in any such applications is to transduce the hybridization events in to a measurable signal with sensitivity, selectivity and speed. The detection techniques most routinely used for the detection of oligonucleotide hybridization, due to physical nature of the readout require the attachment of reporter molecules called "labels" to the target sequences [8].

### 1.1.1 Label-based Detection Mechanisms

Most of the conventionally used oligonucleotide detection mechanisms require 'labels' attached to the target sequences; during read out the amount of labels is detected and assumed to correspond to the number of hybridized target sequences. Labels can be fluorophores, magnetic beads or any such easily detectable materials. A most commonly used detection method is the optical detection technique using fluorescently labeled target

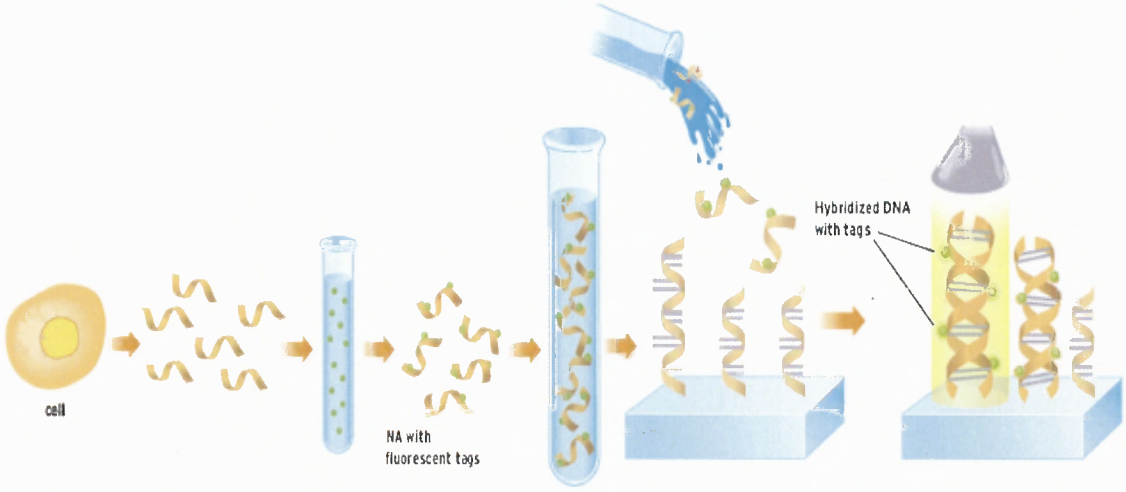


**Figure 1.1** Schematic representation of a fluorescence based optical nucleic acid sensor.

sequences. Figure 1.1 shows schematic of an optical detection mechanism utilizing fluorescently labeled target sequences. Optical detection mechanisms are usually performed in array formats, where, the substrate usually of the size of a microscopic slide or smaller. Onto this substrate are fixed thousands of patches of single stranded nucleic acid probes using the appropriate linkage chemistries. The location and sequence of each patch of oligonucleotide probes are known ahead of time. The target molecules in the sample to be analyzed are labeled with fluorescent tags to aid in the detection. When the tagged single stranded analyte sample is washed over the substrate with the immobilized probes (array), it sticks (hybridizes) fast only to any single-stranded probe sequences that has a complimentary gene sequence to its own. A scan of the substrate or array with a laser or other such excitation source causes any patch of probe sequences that has found a tagged match to fluoresce, and this glow is picked up by a detector which usually consists of charge coupled devices (CCD) [7].

Although this method is well developed and is very sensitive, labeling procedure is complex, time consuming and the detection requires extra sample handling and uses expensive and bulky equipment set-up like confocal microscopes and laser scanner [9, 10]. Labels can also undesirably influence the affinity of the target-probe binding reactions [11]. Also, the need to use conventional organic fluorescent dyes, which suffer from weak signal intensity, photo-bleaching and self quenching limits the span of applications of fluorescence based biosensors [12]. For applications such as point of care diagnostics and other such portable hand-held diagnostic tools which demand fast, inexpensive and relatively simpler monitoring of hybridization, label-free electronic methods are thus highly desirable.

### 1.1.2 Label-free Detection Mechanisms

When the target oligomer sequences hybridize to the probe sequences immobilized on a sensor surface, changes in the electrical (permittivity, resistance), mechanical (mass) and other physiochemical properties occur solely from the presence of the target sequences. Label-free techniques rely on these changes produced as a result of the probe-target interactions and directly transduce them into a measurable signal. These techniques are particularly advantageous due to the fast and inexpensive detection and requirement of no prior sample handling for labeling purposes. Besides the time and expense benefits of omitting the labeling step, label-free techniques can also offer monitoring of hybridization reactions in real-time [13], where as only end-point measurements are performed in the case of label-based methods. Several signal transduction mechanisms such as electrical (capacitive, resistive, field effect), mechanical (micro cantilever based, piezoelectric) and optical (surface Plasmon resonance) have been developed, for the

label-free detection of oligonucleotide hybridization. Mechanical sensors based on micro cantilevers and Quartz crystal microbalance (QCM) related techniques which rely on the mass changes are more suited for protein detection applications due to the higher mass of the protein molecules compared to the nucleic acid sequences. Also, the presence of mechanical motion in the case micro cantilever based sensors offers certain limitations especially for applications requiring massively parallel detection.

Electrical detection techniques based on capacitive sensing mechanisms offer several advantages as a label-free technique due to absence of any mechanical motion and the use of no light. Also due to their low cost, low power consumption and ease of miniaturization capacitive sensors hold great promise for applications where minimizing size and cost is crucial, such as point-of-care diagnostics and biowarfare agent detection.

In this thesis, a novel capacitive sensing mechanism using Gold electrodes with nano-scale electrode separation is presented. The use of nano-scale sensing area offers solutions to several problems suffered by the conventional capacitive detection mechanisms thereby improving the detection sensitivity immensely. In the second part of the thesis the applications and advantages of Field Effect Capacitive sensor with Metal-Oxide-Semiconductor (MOS) architectures, in providing label-free and real-time monitoring of nucleic acid hybridization is demonstrated. Also, a novel Dual parametric capacitive sensor, which encompasses the individual advantages of the above mentioned two sensing architectures on a single sensor, is proposed.

In the final part of the thesis the improvement in the detection speed and selectivity by the use of external electric field is also demonstrated. These detection mechanisms and techniques have the advantage of simplifying the readout and increasing

the speed and ease of nucleic acid assays, which is especially desirable for characterizing infectious agents, scoring sequence polymorphism and genotypes, and measuring mRNA or miRNA levels during expression profiling.

# CHAPTER 2

# CAPACITIVE BIOSENSORS

## 2.1 Conventional Capacitive Biosensors: Limitations

Among the various label-free signal transductions mechanisms that have been investigated for monitoring biomolecular interactions, capacitive sensors receives special attention, due to several advantages such as simple instrumentation, absensence of any moving parts as well as its easiness for multiplexing in view of high throughput applications [14]. Non-Faradaic impedance spectroscopic measurements conducted on capacitive structures has been regarded as a versatile analytical tool for studying and detecting binding/hybridization events due to its ability to investigate the relaxation processes occurring in an extremely wide range of characteristic times (wide range of frequencies).The detection is based on the changes in the sensor capacitance or permittivity as a result of the probe-target binding.

Although, several configurations of capacitive biosensors for such applications have been reported in the literature, many physical and electrochemical properties of these structures and the measurement methods used have significantly limited its ability to provide enough sensitivity and other attributes required to be developed as a reliable biosensing mechanism: Firstly, there is a strong polarization in the vicinity of the electrodes which results in huge impedance due the electrical double layer and can in turn dwarf the dielectric property changes due to biomolecular interactions. Secondly, the aqueous (electrolytic solution) sample usually displays a very high ionic electrical conductivity and causes a giant frequency-dependent dielectric dispersion. This parasitic effect associated with the conductivity of the buffer solution in fact masks the dielectric

relaxations of interest associated with the biomolecules in the sample. These effects are more pronounced in the low frequency tail of the impedance (dielectric) spectrum. Due to this reason, traditional capacitive sensing mechanisms were analyzed using impedance spectroscopic measurements at higher frequencies which offered reduced sensitivity towards biomolecular interactions as the applied excitation signals were too fast for the charged bio-macromolecules to respond.

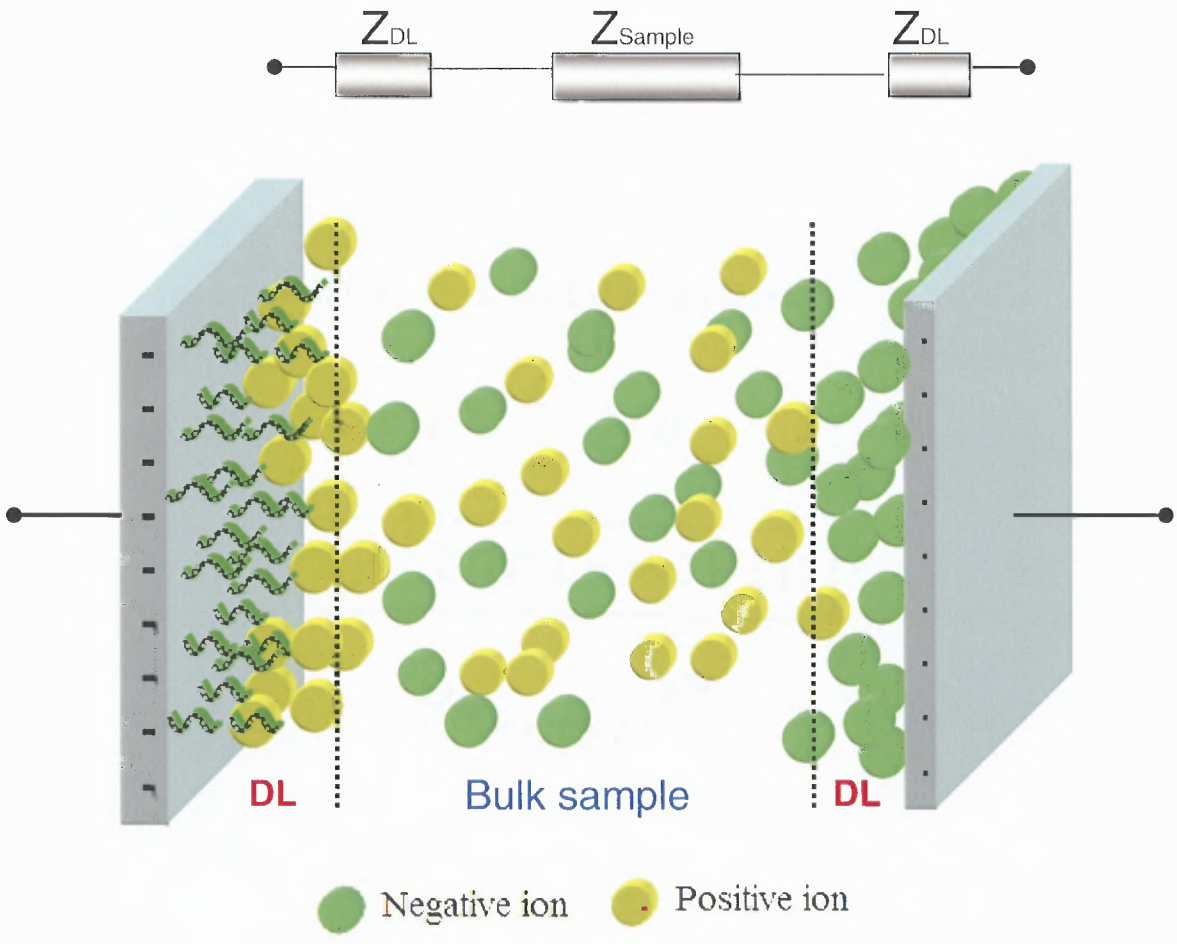


**Figure 2.1** Schematic representation of conventional capacitive biosensor showing the electrical double layers formed due to the accumulation of ions near the electrode surface. The impedance due to this polarization effect is more pronounced at low frequencies and hence masks the dielectric permittivity changes due to biomolecular interactions. This is a major cause for the limited sensitivity of such devices.

Figure 2.1 shows a Schematic representation of the conventional capacitive biosensor showing the electrical double layers formed due to the accumulation of ions near the electrode surface. At low frequencies the series parasitic impedance due to the electrical double layers will be more pronounced and masks any capacitance (dielectric property) changes resulting from biomolecular interactions.

Impedance Spectroscopy of Nucleic Acid Molecules in General

Impedance or dielectric spectroscopy is one of the most commonly used analytical tools for studying the structure and dynamics of polyelectrolyte solutions. Its ability to investigate the relaxation processes occurring in an extremely wide range of characteristic times (roughly from $10^{-12}$s to $10^{3}$s) make it versatile tool for revealing information about electron transfer, atomic bonds, and large-scale molecular structure of the polymer solutions [15-18]. The characteristic time scale ranges from $10^{-12}$s for electrons, $10^{-9}$s for atomic bonds, to $10^{-3}$s for molecular structures. Therefore, when an oscillatory field excites molecules in a sample they respond differently depending on the frequency. The large- scale molecular structural changes such as the changes occurring during hybridization (single stranded to double stranded structure) are revealed during the low frequency responses. The dielectric response of DNA solutions has been widely studied [19-26]. The dielectric relaxation of Nucleic Acid solution occurs mainly at 3 different frequency regions: $\alpha$ (near DC to a few kHz frequency range) $\beta$ (around 1 MHz to 1 GHz) and $\gamma$ (above 1GHz). Among these $\alpha$ relaxation is found to be the most useful for information regarding the structure and the length of the molecules. In other words low frequency (near DC to a few kHz frequencies) dielectric measurements are more sensitive towards Nucleic Acid hybridizations or any such biomolecular interactions. The

relaxation reflects the migration of counter ions over the charged oligonucleotide sequences and hence it closely related to the electrochemical double layer at the vicinity of the electrodes. The impedance due to the double layer dominates the measured capacitance at low frequencies (<1 kHz) and hence masks the dielectric property changes resulting from the hybridization of the probe and target sequences.

## 2.2 Electrode Polarization or the Electrical Double Layer Effect

Electrode polarization effect due to the spatial charge that accumulates near the electrode surface represents a major cause of reduction in the sensitivities of the traditional dielectric spectroscopic measurements for biomolecular analysis and detection. The presence of this "double layer" of charge modifies the field distribution with the anlyte solution. This debilitating effect can be approximately modeled as surface impedance comprising mainly of capacitance in series with the sample impedance [27-30]. As the thickness of the electrical double layers are usually very low (nanometer range) the impedance provided by this electrical double layer capacitance is huge and its presence makes it difficult if not impossible, to resolve the dielectric dispersion at lower frequencies. More over, the presence of this undesired impedance will mask the dielectric property changes or increment occurring as a result of the biomolecular interactions leading to the reduced sensitivity of the traditional capacitive sensing architectures. Several approaches and strategies have been proposed over the years to cope with this problem.

The various approaches that have been proposed to correct the limitations caused by the electrode polarization effects [16] can be roughly categorized by their nature in to

two. The first category includes the method that have been proposed and been tried to eliminate or reduce the impact of the effect. The second category comprises of methods that have been proposed and devised to correct the measured dielectric spectra by modeling the effect as the presence of surface impedance.

The methods proposed to eliminate or reduce the impact of the electrode polarization includes approaches such as the four electrode method [18, 31, 32], and the electromagnetic induction method [33, 34]. The four electrode method utilizes the observation that the electrochemical double layer builds up at the surface of the two current electrodes, but not on the two inner high-impedance voltage sensing electrodes, as in the case of these electrodes the input current is virtually zero. In the case of the electromagnetic induction method, the voltage and the current electrodes are replaced by two toroidal coils and the complex permittivity is deduced from the measured coupling of the two coils. Increasing the surface area of the capacitive electrodes is another effective method which has been using to reduce the effect of the electrode polarization. The use of electrode with large surface area reduces the capacitive impedance produced due to the double layer capacitance. The use of micro porous electrodes has been demonstrated to increase the effective surface area of the electrodes by a factor of 100- 1000 times with respect to the geometrical surface area of the electrodes. For example, by depositing a layer of 'platinum black' (electro-deposited colloidal platinum), the effective surface area of the electrodes can be substantially increased [35, 36].

A commonly used method for correcting the measured dielectric spectrum from the effects of the electrode polarization is the taking of the dielectric measurements at different electrode spacings [16, 37-40]. This approach is based on the assumption that

the polarization impedance does not depend on the electrode spacing. Since the sample impedance on the other hand depends on the electrode spacing, it is proposed that the contribution from the electrode polarization can be eliminated from a set of measurements at two different electrode spacing. In practice, the capacitance at each frequency is linear in reciprocal electrode spacing and extrapolated to 1/d =0 to obtain the sample capacitance [40]. Mandel and co-workers used similar method to determine the low-frequency spectroscopic data.

Another major method referred to as the substitution method [24, 35, 41, 42], the electrode polarization impedance is eliminated by means of calibration with sample electrolytes of known conductivity. This method is based on the assumption that the polarization effects are same in the case of the electrolyte used for calibration and in the case of the sample solution. Although many such methods have been proposed, an entirely satisfactory solution for the problem of reducing the electrode polarization effect is not known. Also, none of the above proposed techniques for eliminating and also for correcting the errors due to the electrode polarization effect, was compatible with the biosensing applications.

# CHAPTER 3

# GOLD NANO-CAVITY CAPACITIVE SENSORS

## 3.1 Elimination of Electrode Polarization Effect Through Double Layer Overlapping in Nano-cavity Capacitive Sensors

In an attempt to minimize or even eliminated, the errors due to the electrode polarization effect a novel capacitive sensor with nano-scale electrode spacing is proposed. The huge impedance of the electrical double layer is formed due to the accumulation of counter ions on the electrode surface which is in contact with the electrolyte [43]. When the electrode separation is reduced below the characteristic length of this diffuse double layer of charges (Debye length), the electrical double layers interact and overlap each other due to the space confinement. Such interactions are expected to minimize or even eliminate the contribution of double layer impedance (electrode polarization effect) in the measured capacitance. The impedance spectra of DI water and electrolyte solutions of various ionic strengths obtained using these nano-scale dielectric sensors confirms this effect. This concept is theoretically verified by solving the PB equation for the electrical potential and ion distribution with in the nano-scale cavity.

## 3.2 Calculation of the Electrical Double Layer Width: Debye Length

The thickness of the electrical double layer is the reciprocal of the Debye-Hückel parameter, $\kappa$ [43]. In an electrolyte or a colloidal dispersion the Debye length is usually denoted by the symbol $\kappa^{-1}$

$$\kappa^{-1} = \sqrt{\frac{\varepsilon_0 \varepsilon_r kT}{2N_A e^2 I}} \tag{3.1}$$

Where

$I$ is the ionic strength of the electrolyte (SSC buffer solution).

$\varepsilon_0$ is the permittivity of the free space = 8.85 x $10^{-12}$ $C^2N^{-1}m^{-2}$.

$\varepsilon_r$ is the relative permittivity of the electrolyte solution = 60 ~80 (assumed to be less than $\varepsilon_r$ of water).

$k$ is the Boltzmann's constant = 1.38 x $10^{-23}$ $JK^{-1}$.

$T$ is the absolute temperature in Kelvin = 298 K.

$N_A$ is Avogadro's number = 6.023 x $10^{23}$.

$e$ is the elementary charge = 1.602 x $10^{-19}$ C.

Ionic strength of solution is a measure of the concentration of all ions present in that solution

Ionic strength,

$$I = \frac{1}{2}\sum_{B=1}^{n} c_B z_B^2 \tag{3.2}$$

For calculating the ionic strength of 0.05xSSC buffer (0.0075M Sodium Chloride and 0.00075M Sodium Citrate)

$$I = 1/2\,[(+1)^2 * 0.0075 + 3\,\{(+1)^2 * 0.00075\} + (-1)^2 * 0.0075 + (-3)^2 * 0.00075]$$

$$= 0.012 \text{ M} = 0.012 \text{ moles/liter} = 12 \text{ mol/m}^3$$

Substituting the following values in the equation (3.1)

Double layer width (Debye length) $\kappa^{-1}$ = 2.8 nm

### 3.3 Theoretical Model for the Overlapped Electrical Double Layer Fields

When the separation between the capacitive electrodes is reduced to scale of the calculated width of the electrical double layers (Debye length), their double layers will overlap and interact with one another. The ionic distribution in the electrolyte at the vicinity of the electrode is first predicted by Gouy (1910) and Chapman (1913) utilizing Poisson-Boltzmann (PB) equation. Such an interaction is expected to reduce the potential drop across the double layers. For studying the overlapped EDL fields, the classical treatment involves application of the Poisson-Boltzmann equation, which is a combination of the Poisson equation and the Boltzmann equation. The assumptions and approximations involved in the derivation of the Boltzmann equation involves the treatment of the aqueous phase to be infinitely large, so that the electrical potential in the liquid far away from the charged electrode surface is zero and that the ionic concentrations in the liquid far away from the capacitive electrode is equal to the concentration of the original bulk solution [44].

A theoretical model to evaluate the electrical potential distribution in an overlapped electrical double layer region was first developed by Verwey and Overbeek [45-47], based on the Gouy-Chapman EDL theory. For the simplicity of analysis Verwey and Overbeek's model was developed for an overlapped double layer field between two infinitely large flat electrodes that have the same surface potential. When the two double layers overlap, the electrical interaction will change the distributions of the electrical potential and the ions across the capacitive regions. The redistribution of the electrical potential in the interacted double layer regions in shown in the Figure 3.1.

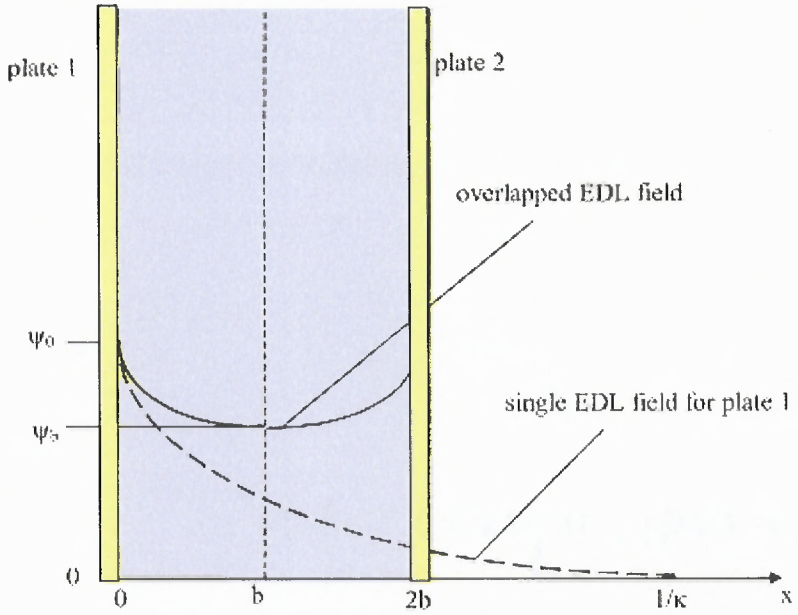


**Figure 3.1.** Schematic description of the electrical potential distribution in the overlapped EDL field between two electrodes with nano-scale separation. $\Psi_0$ is the electrical potential at the surface, $\Psi_b$ is the potential at the middle plane, $2b$ the separation distance between the electrodes, and $1/\kappa$ the width of the single electrical double layer.

For the simplicity of the electrical calculation, the electrodes are assumed to be infinitely large and hence the electrical double layer fields between them are one dimensional. The coordinate system used for the calculation is as shown in the figure. The electrolyte solution is assumed to be symmetric (1:1) salt solution such as KCl or NaCl. The fundamental electrostatic equation for such a system which describes the relationship between the electrical potential $\psi$ and the net charge density per unit volume $\rho_e$ at any point in the sample.

$$\frac{d^2\psi}{dx^2} = -\frac{\rho_e}{\varepsilon} \tag{3.3}$$

Where $\varepsilon$ is the dielectric constant of the sample.

Considering that the system is in equilibrium, the electrochemical potential of the ions should be constant everywhere; that is,

$$\frac{d\bar{\mu}_i}{dx} = 0 \tag{3.4}$$

Where $i$ denotes the type $i$ ions and the electrochemical potential $\bar{\mu}_i$ is defined as

$$\bar{\mu}_i = \mu_i + z_i e\psi \tag{3.5}$$

Where $\mu_i$ and $z_i$ are the chemical potential and the valence of the type-$i$ ions, respectively; $e$ is the charge of a proton. The chemical potential of the ions can be further expressed as

$$\mu_i = \mu_i^{\,0} + k_b T \ln n_i \tag{3.6}$$

where $\mu_i^{\,0}$ is a constant for the type-$i$ ions, $k_b$ is the Boltzmann constant, $T$ is the absolute temperature of the sample, and $n_i$ is the number concentration of the type-$i$ ions. Substituting Equations (3) and (4) into equation (2) yields

$$\frac{1}{n_i}\frac{dn_i}{dx} = -\frac{z_i e}{k_b T}\frac{d\psi}{dx} \tag{3.7}$$

Integrating equation (5) from a point in the bulk solution where

$$x = \infty, \ \psi = 0 \ \text{and} \ n_i = n_i^{\,0} \tag{3.8}$$

to a point in the EDL region. $n_i^{\,0}$ in equation (6) is the bulk concentration of the type-$i$ ions. This leads to the Boltzmann equation,

$$n_i = n_i^{\,0} \exp\left(-\frac{z_i e\psi}{k_b T}\right) \tag{3.9}$$

The net charge density per unit volume $\rho_e$ is proportional to the local concentration difference between cations and anions. For a 1:1 symmetric electrolyte solution, we have

$$\rho_e = e(n_+ - n_-) = -2en^0 \sinh\left(\frac{e\psi}{k_b zT}\right) \tag{3.10}$$

Where, $z_+ = z_- = 1$, $n^+ = n^- = n^0$. Substituting equation (7) and (8) into equation (1) leads to the well known Poisson-Boltzmann equation

$$\frac{d^2\psi}{dx^2} = \frac{2en^0}{\varepsilon} \sinh\left(\frac{e\psi}{k_b T}\right) \tag{3.11}$$

In Verwey and Overbeek's model of the overlapped EDL fields [48] the Poisson-Boltzmann equation was applied to the system as shown in the figure 4. with the following boundary conditions.

$$\psi\big|_{x=0} = \psi_0 \tag{3.12}$$

$$\left.\frac{d\psi}{dx}\right|_{x=b} = 0 \tag{3.13}$$

Where $\psi_0$ indicates the electrical potential at the surface. If $\psi$ is small, and $e\psi/k_bT < 1$, the right hand side of the equation (3.11) can be simplified by using the approximation,

$$\sinh x \approx x \text{ when } x \text{ is small.}$$

Therefore, equation (3.11) can be written as

$$\frac{d^2\psi}{dx^2} = \frac{2e^2n^0}{\varepsilon k_b T}\psi \tag{3.14}$$

The above simplification is referred to as the Debye-Hückel approximation. If a parameter $\kappa$ is defined as

$$\kappa = \left(\frac{2e^2n^0}{\varepsilon k_b T}\right)^{\frac{1}{2}} \tag{3.15}$$

Equation (3.14) can be further simplified as

$$\frac{d^2\psi}{dx^2} = \kappa^2\psi \tag{3.16}$$

$\kappa$ is referred to as the Debye-Hückel parameter. 1/ $\kappa$ is normally referred to as the characteristic thickness of the electrical double layer. Equation (3.16) together with the boundary conditions, equation (3.12) and (3.13) can be solved and the solution predicts the potential distribution in the overlapped double layer region as follows:

$$\psi(x) = \psi_0 \frac{\cosh(\kappa(b-x))}{\cosh(\kappa b)} \tag{3.17}$$

Once the potential distribution id determined, the ion concentration distribution can be obtained from the Boltzmann equation, Eq. (3.9). Under the Debye-Hückel approximation, the Boltzmann equation can be further simplified as

$$n_+ = n^0\left(1-\frac{e\psi}{k_bT}\right) \tag{3.18}$$

$$n_- = n^0\left(1+\frac{e\psi}{k_bT}\right) \tag{3.19}$$

### 3.4 Electrical Potential Distribution with in Various Electrode Separations

The electrical potential distribution in between the capacitive electrodes for three different electrode separations are simulated using MATLAB and is illustrated in figures 5, 6 and 7. The graph shows calculated potential distributions for capacitive architectures

with $2b\kappa = 1, 4$, and 20, where 2b is the separation between the electrodes and $1/\kappa$ is the width of the double layer (Debye length). Utilizing the symmetry of the distribution with respect to the electrodes only the distribution from one electrode surface to the middle of the sample is shown. Figure 5 shows the distribution of electrical potential from one of the capacitive electrodes to the center of the sample when the electrode separation is equal to the double layer width.

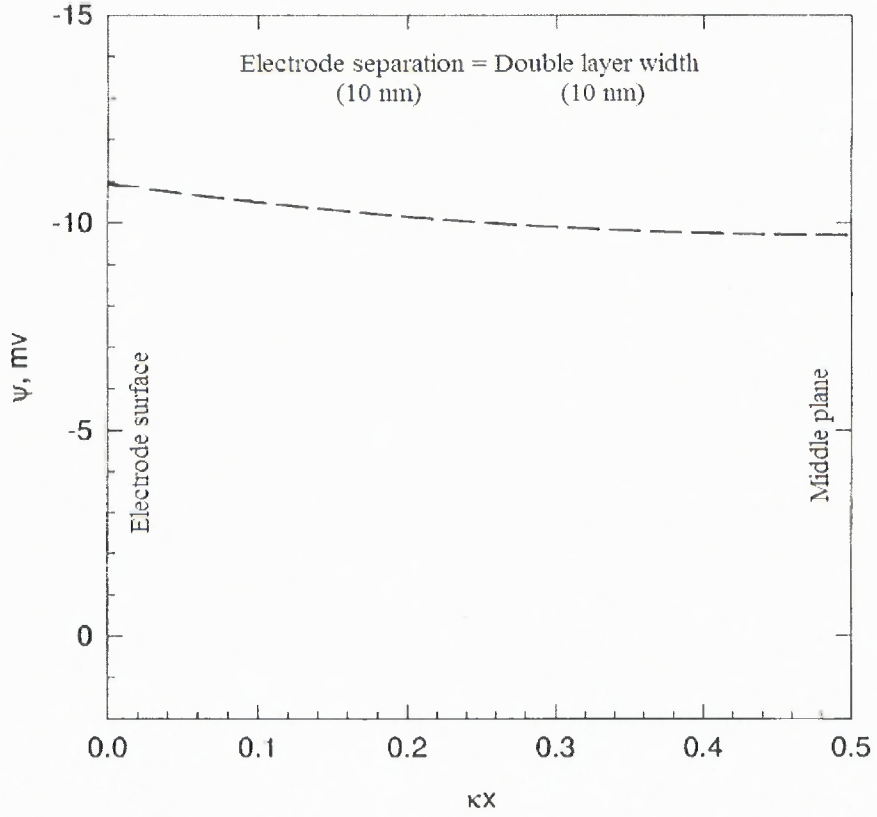


**Figure 3.2** Electrical potential distribution in between capacitive electrodes with electrode separation equal to the double layer width, $2b\kappa = 1$.

Considering a case of electrical double layer width being say 10 nm, figure 5 shows the potential distribution between the capacitive electrodes with 10 nm electrode separations.

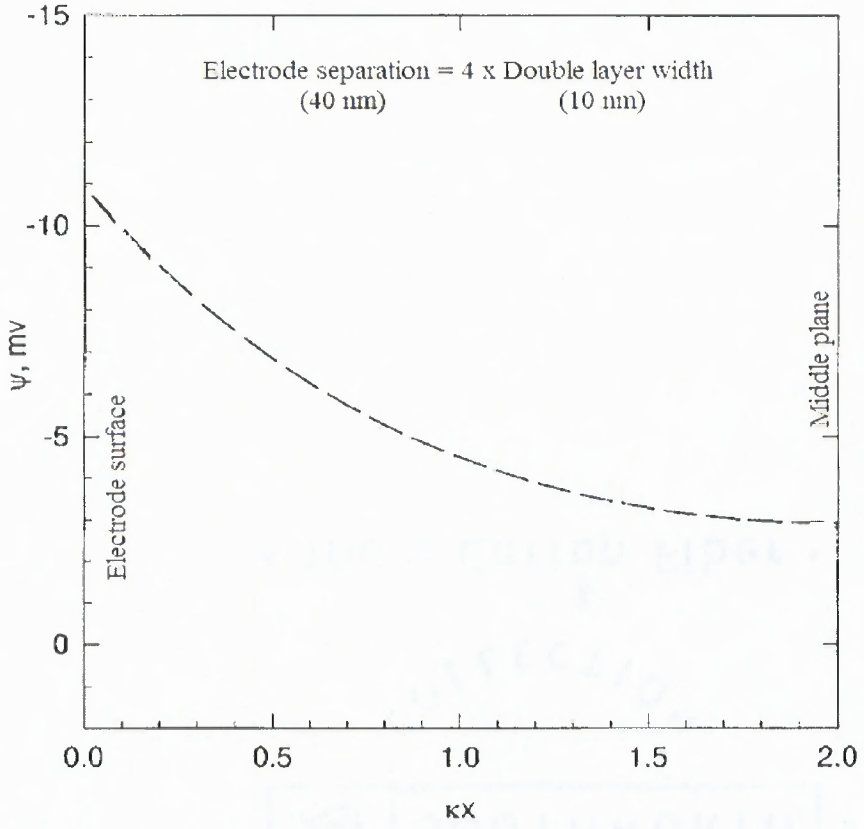


**Figure 3.3** Electrical potential distribution in between capacitive electrodes with electrode separation equal to four times the double layer width, $2b\kappa = 4$.

The distribution of electrical potential between the capacitive electrodes with a separation four times the double layer thickness is shown in figure 6. In this case for the assumed double layer width of 10nm the electrode separation is 40 nm. Figure 7 shows the electrical potential distribution between the capacitive electrodes when the separation is 20 times the double layer thickness. This is a case of having an electrode separation of 200 nm with a electrolyte sample of double layer width 10 nm. The graphs show that when the separation between the capacitive electrodes is comparable to or smaller than the electrical double width, the potential difference between the electrode surface and the

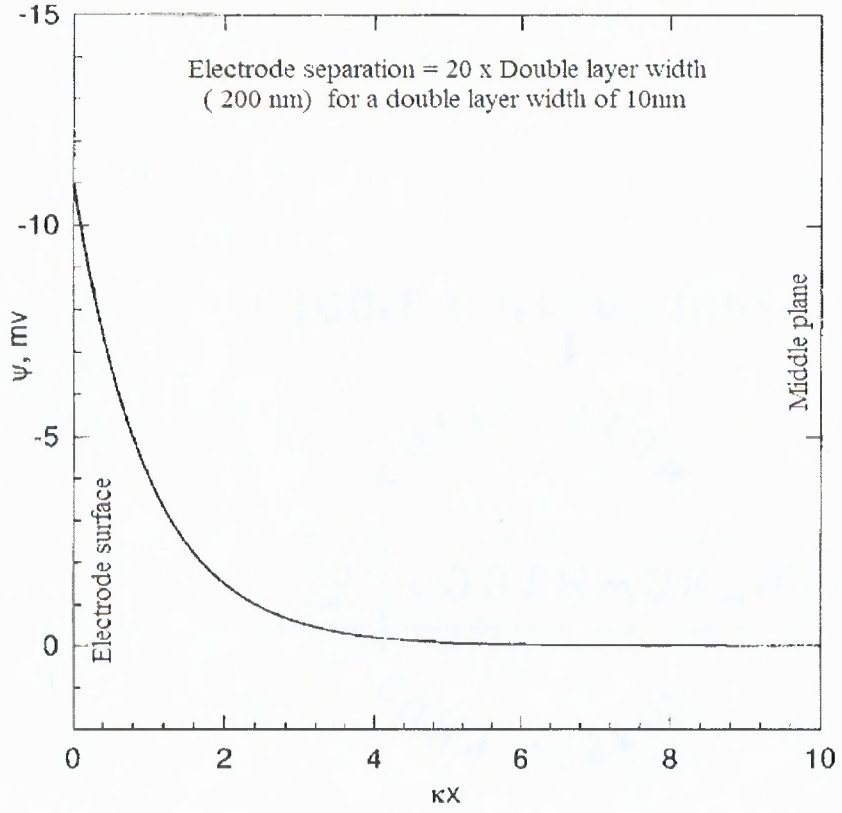


**Figure 3.4** Electrical potential distribution in between capacitive electrodes with electrode separation equal to twenty times the double layer width, $2b\kappa = 20$.

middle plane of the sample solution is reduced. This clearly indicates that as the electrode separation is reduced the effect of the electrical double layer impedance on the applied excitation signal is minimized.

## 3.5 Device Fabrication

The most critical parameter for enhancing sensitivity by eliminating the electrode polarization effect is the nanometer separation between the capacitive electrodes. The desired separation of less than 50nm is difficult to achieve with the conventional lithographic techniques [49]. To overcome the resolution limit, we have used a sacrificial

layer process, where the thickness of the $SiO_2$ spacer film determines the electrode separation. The process steps are schematically indicated in Figure 3.5.

In the first process step 500nm thick Silicon Nitride is deposited on the single side polished <100> Si wafer followed by the patterning of 1μm thick photo resist spacers to act as the sacrificial layer for the formation of the first set of Au electrodes (a). Gold electrodes are deposited using E-beam evaporation under ultra high vacuum conditions. The selective removal of the photo resist sacrificial layer defines the first set of Au electrodes (b).

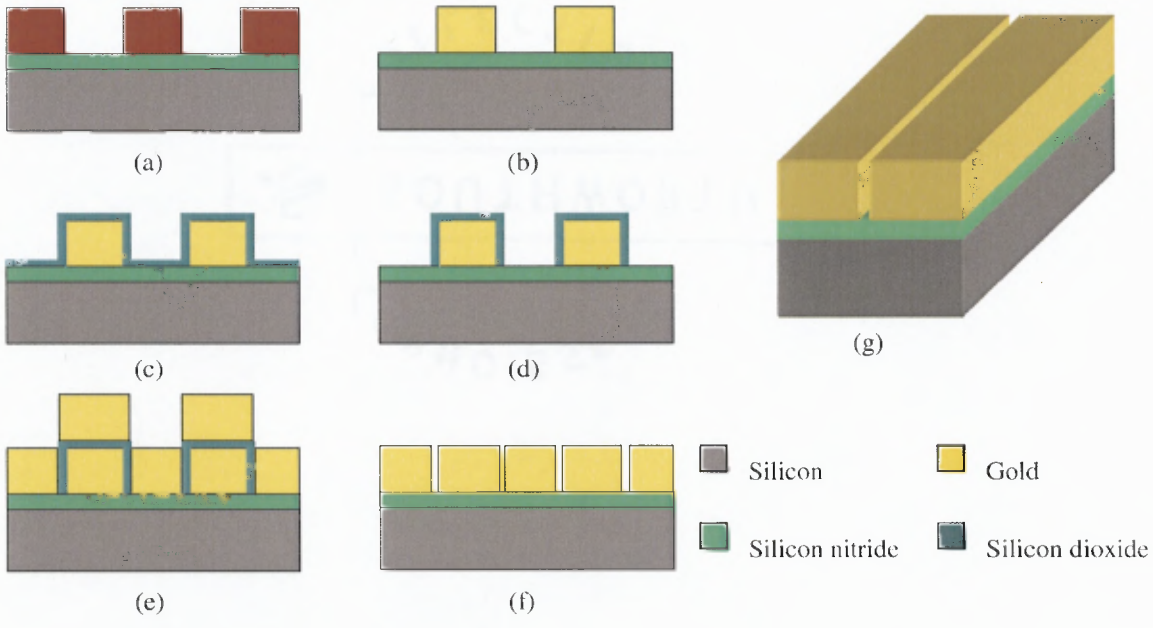


**Figure 3.5** Schematics of the fabrication process flow (a) photo resist spacers are patterned (b) gold electrodes formed by sacrificial method (c, d) deposition and patterning of $SiO_2$ for nanometer spacing (e) deposition of gold (f) $SiO_2$ spacer removal (g) a nano-cavity capacitive sensing structure.

In the next step a very thin and uniform layer of SiO2 is deposited using Plasma Enhanced Chemical Vapor Deposition (PECVD), to form the nanometer spacers between

the electrodes (c). Followed by the patterning of SiO2 sacrificial layer, a second layer of gold metallization of 1μm is done using E-beam evaporation (d). Finally the $SiO_2$ spacer film between the gold electrodes is selectively etched off using HF (e). The deposited Silicon Nitride layer will act as etch stop of this etching process and also serves as an isolator between the gold electrodes and the Si wafer. Here the use of deposited oxide thin film to define the separation between gold electrodes allows the fabrication of capacitive structures with electrode separations lower than the resolution limit of optical or e-beam lithography.

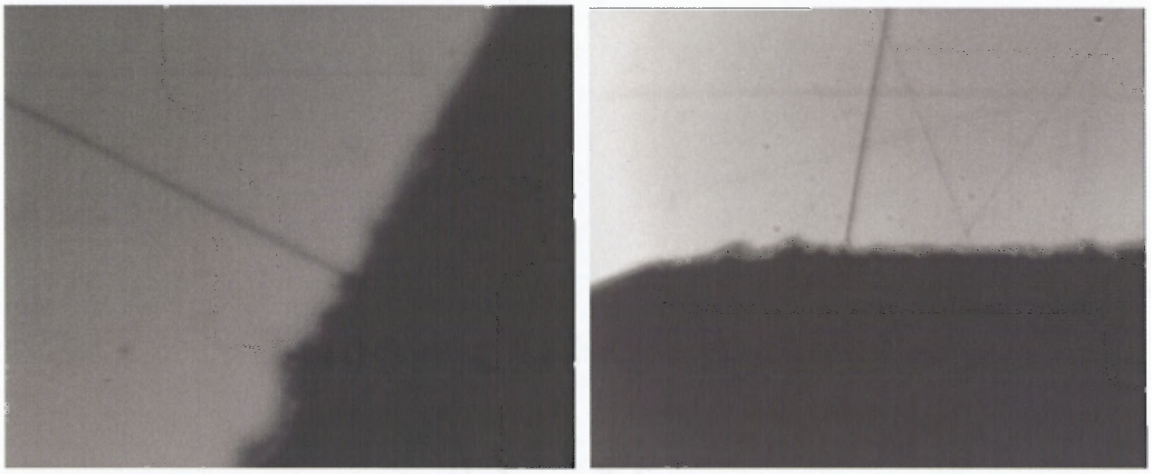

**Figure 3.6** Microscopic images of Au electrodes with nano-scale separation.

## 3.6 Measurement Setup and Calculation of Complex Permittivity from the Transfer Function

The dielectric property changes due to hybridization are probed using a Fast-Fourier Transform (FFT) spectrum analyzer. The dielectric properties were investigated over a frequency range of 10Hz to 100 kHz, with 0V DC bias and 20mV AC signals using an SR 785, 2 channel dynamic signal analyzer. A Lab View program was used to collect and

record data through a GPIB interface. An external Op-Amp amplifier circuit is used to further minimize the noise. Figure 3.7 shows actual measurement system used for the impedance spectroscopic measurements.

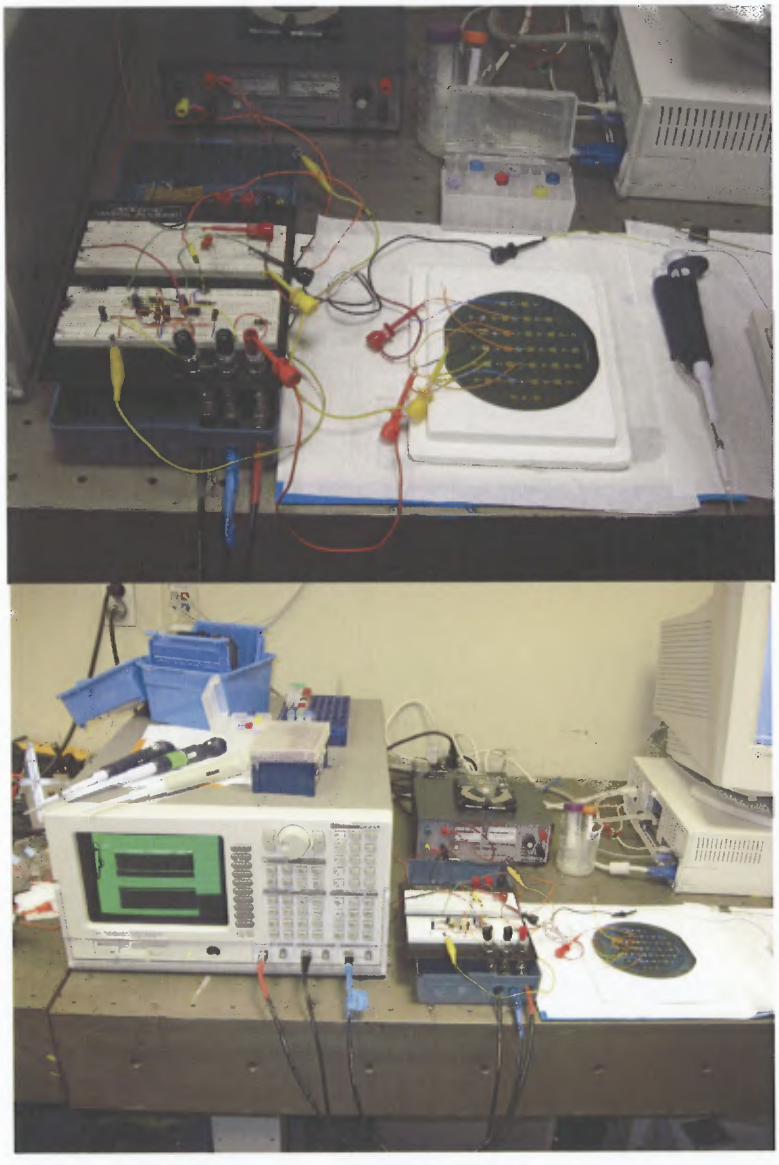

**Figure 3.7** Actual measurement system used for the dielectric spectroscopic measurements on the nano-cavity capacitive sensors.

Figure 3.8 shows the schematics of the measurement set up used. The ac voltage applied to the electrodes produces both conduction current and a displacement current through the sample. The real and imaginary parts of the transfer function $V_2(\omega)/V_1(\omega)$ are proportional to the conductivity and the dielectric constant, respectively. The output of the signal analyzer is applied to one of the capacitive electrodes through $R_1$. The other electrode of the capacitive sensor is connected to the negative input of the amplifier $A_2$, which holds the electrode at ground potential. As a result the current I that flows through the nano-cavity sensor produces a voltage $V_2$ which is equivalent to the product of I and the sample impedance Z. The value

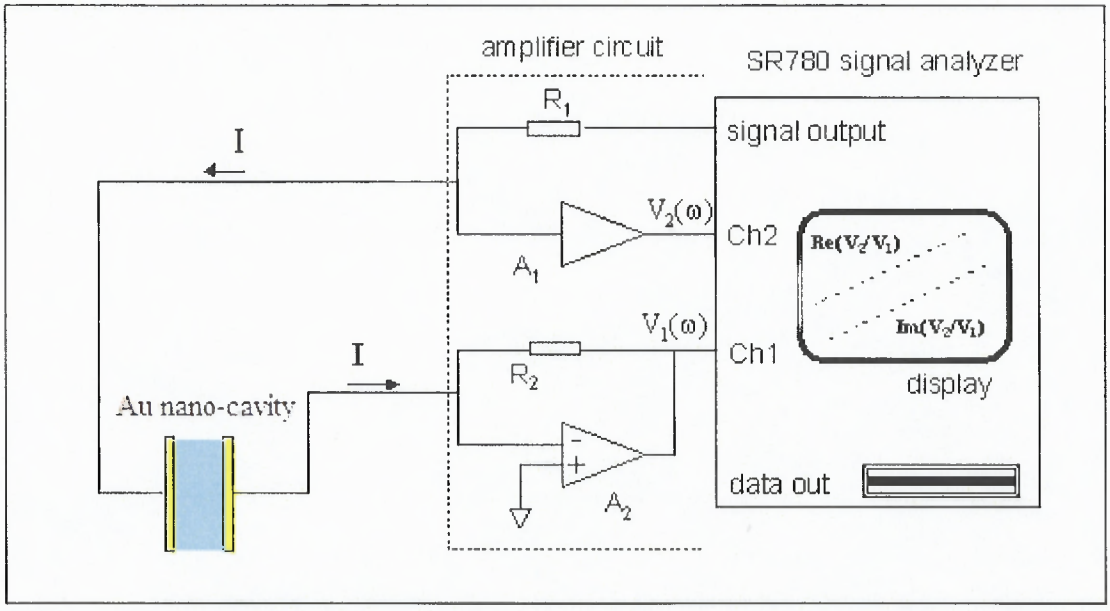


**Figure 3.8** Experimental setup for performing the dielectric spectroscopic measurements on nano-cavity capacitive sensors. An external amplifier circuit is designed and implemented to reduce noise.

of voltage drop $V_1$ is equal to the product of I and $R_2$. Thus the transfer function of the system is given by,

$$\frac{V_2(\omega)}{V_1(\omega)} = \frac{Z}{R_2} \tag{3.20}$$

where $Z$ is the overall impedance of the sample. The transfer function is denoted by $T(\omega)$ or $T$ for the rest of the calculations. The purpose of $R_1$ is to provide an upper limit for the current $I$ as the impedance $Z$ becomes smaller at higher frequencies. The unity gain amplifier $A_1$ provides buffering so that the input impedance of Channel 2 does not affect the voltage drop across the sample.

For deducing the dielectric permittivity of the sample in between the nano-cavities, the sensor is represented by an equivalent circuit as shown in the Figure 3.9.

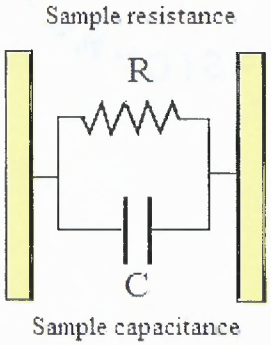


**Figure 3.9** Equivalent circuit representation of the nano-cavity capacitive sensor. R represents the resistance of the bulk sample and C the capacitance between the places.

From equation (3.20) the total impedance Z of the sample is given by

$$Z = T \times R_2 \tag{3.21}$$

From the equivalent circuit of the sample

$$\frac{1}{Z} = \frac{1}{R} + iC\omega \tag{3.22}$$

Substituting in equation (3.21)

$$\frac{1}{TR_2} = \frac{1}{R} + iC\omega \tag{3.23}$$

$$\Rightarrow \mathrm{Im}\left(\frac{1}{TR_2}\right) = C\omega$$
$$\Rightarrow \mathrm{Im}\left(\frac{1}{TR_2\omega}\right) = C \tag{3.24}$$

The capacitance C can also be expressed as

$$C = \frac{\varepsilon_0 \varepsilon_r A}{d} \tag{3.25}$$

Where, $\varepsilon_0$ is the absolute permittivity,

$\varepsilon_r$ is the relative permittivity of the sample,

$A$ is the area of the capacitive electrode surface and

$d$ is the nano-scale distance between the electrodes.

Combining equation (3.24) and (3.25) and solving for $\varepsilon_r$,

Sample permittivity, $$\varepsilon_r = \mathrm{Im}\left(\frac{d}{TR_2\varepsilon_0 A\omega}\right) \tag{3.26}$$

Complex permittivity $$\hat{\varepsilon} = \varepsilon' - i\varepsilon'' \tag{3.27}$$

where $\varepsilon' = \varepsilon_r$ is the relative permittivity of the sample, and $\varepsilon''$ is the dielectric loss of the sample.

To calculate $\varepsilon''$ from the measured transfer function, considering the real part of Eq. (3.23)

$$\mathrm{Re}\left(\frac{1}{TR_2}\right) = \frac{1}{R} \tag{3.28}$$

Resistance of the sample can also be expressed as

$$R = \frac{d}{\sigma A} \tag{3.29}$$

where $d$ is the distance between the electrodes, $\sigma$ is the conductivity of the sample and $A$ is the area of the capacitive electrodes. The conductivity of the sample can be expressed in terms of dielectric loss and the frequency of the excitation signal as

$$\sigma = \varepsilon'' \omega \tag{3.30}$$

Combining equation (3.29) and (3.30) together and substituting in equation (3.28) for R gives,

$$\mathrm{Re}\left(\frac{1}{TR_2}\right) = \frac{\varepsilon'' \omega A}{d} \tag{3.31}$$

Solving equation (3.31) for ε" gives,

Dielectric loss of the sample $$\varepsilon'' = \mathrm{Re}\left(\frac{d}{TR_2 A \omega}\right) \tag{3.32}$$

Hence from the transfer function $T(\omega)$ obtained from the signal analyzer the relative permittivity and the dielectric loss of the sample can be calculated as

Dielectric loss of the sample, $$\varepsilon'' = \mathrm{Re}\left(\frac{d}{TR_2 A \omega}\right) \tag{3.33}$$

Relative permittivity of the sample, $$\varepsilon_r = \mathrm{Im}\left(\frac{d}{TR_2 \varepsilon_0 A \omega}\right) \tag{3.34}$$

A MATLAB program is used to implement the above equations and obtain the relative permittivity and the dielectric loss from the signal analyzer output.

### 3.7 Dielectric Spectrum of Various Concentrations of Buffer Solutions

The electrical contacts and the functioning of the entire system including the capacitive element were verified by measuring the dielectric spectrum with air and De Ionized water

in between the electrodes. The relative permittivity of the samples were calculated from the transfer functions as described above and verified with the known values. Before conducting the biomolecualar detection experiments, the response of the sensor to various concentrations of the buffer solutions was tested to study the properties to the double layer. The order of introducing the solutions were from DI water to monotonically increasing concentrations of buffer, in order to avoid any errors due to fluid left over from previously tested higher concentration. A volume of 0.2 μl of each of the fluid were pipette on to the sensor and the remaining fluid and the fluid from the cavities after taking the spectrum was removed using a small strip of lint-free absorbent paper.

### 3.8 Immobilization and Hybridization Procedures

DNA oligonucleotides including the thiol labeled probe sequences used for the experiments were purchased from IDT (Integrated DNA Technologies). 20xSSC buffer solution (3.0M Sodium Chloride + 0.3M Sodium Citrate) used for the hybridization assay was purchased from Sigma-Aldrich. The chemicals and other materials used for microfabrication of the device were obtained from Microfabrication Center at New Jersey Institute of Technology. Single stranded DNA sequences pre-modified by the thio linker (5'-CACGTAGCAG/3Thio MC3-D/-3') were immobilized on the gold metal gate using a concentration of 10uM in 0.05xSSC buffer. By taking advantage the high affinity of sulphur atoms to gold substrate the DNA molecules with thiol end groups are chemically assembled onto the gold surface from the solution [50, 51]. The oligomer chains are thus tethered to the gold substrate at one end and the rest of the chain stays fully extended at an angle of approximately 30 degree from the surface.

The Van der Waals forces between adjacent chains helps to order the oligomers parallel to each other [52]. The <111> crystal orientation of gold which is obtained by thin film deposition of gold on SiO2 is found to give excellent result for the formation of self assembled monolayers (SAM) [53]. Mercapto hexanol (HS- (CH2)6 OH ) SAM layers were immobilized in between the DNA strands in order to passivate the vacant spaces. Mercaptohexanol layer would also help in providing an upright position for the oligomers due to electrostatic repulsion. Prior to immobilization procedure the structure was cleansed using acetone, isopropanol and deionized water. The substrates with immobilized oligomers were then allowed to interact with complementary oligomers (5'-CTG CTA CGT G-3') of concentrations from 0.1μM to 10μM over a short period of time. After incubation, the substrates were rinsed with deionized water to remove the nonspecifically bound target molecules.

### 3.9 Results and Discussion

The results of the dielectric spectroscopic measurements with air and De-Ionized water between the capacitive electrodes are shown in the Figure.3.10. The observed relative permittivity of DI water less than 80 can be explained by the presence of unfilled air gaps between the nano-space cavities. The dielectric spectrum of various concentrations of the SSC buffer used is shown in Figure 3.11. The measured capacitance (relative permittivity) is found to be not significantly influenced by the ionic strength of the solution. This is extremely beneficial in using the sensors for studying and detecting the dielectric property changes due to the presence of biomolecules.

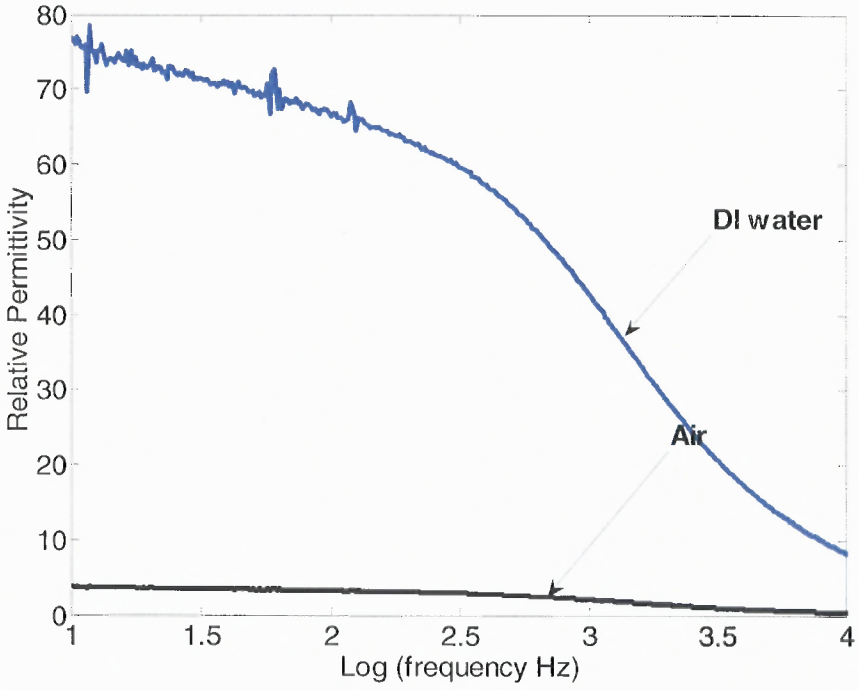


**Figure 3.10** Dilelectric spectrum of Air and DI water between the capacitive electrodes.

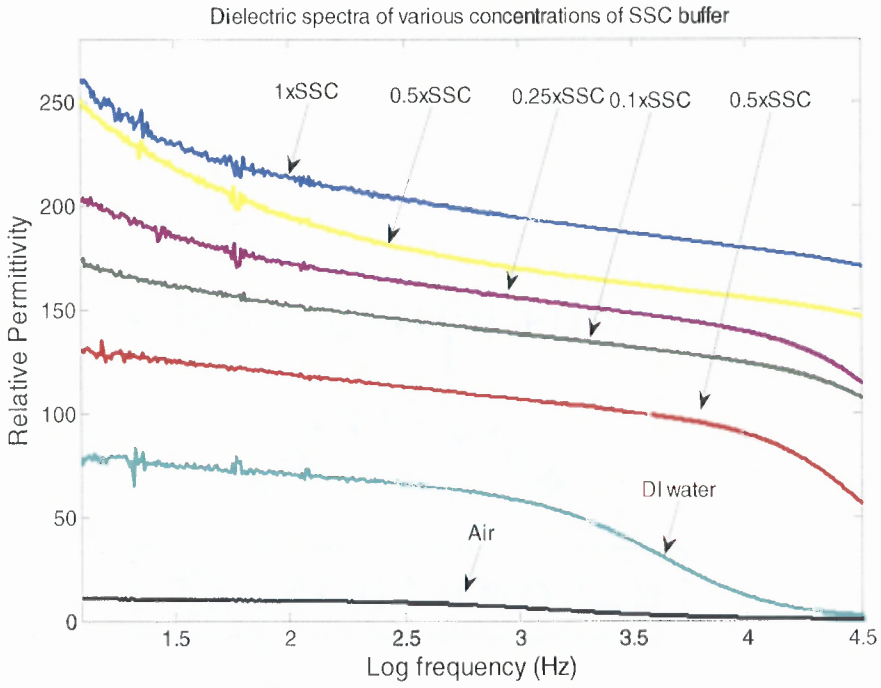


**Figure 3.11** Relative permittivity as a function of frequency for various concentrations of buffer solutions. The measured permittivity is found to be not significantly influenced by the ionic strength of the solution.

This observation can be accounted by two competing effects happening in the sensor as a result of the increase in the salt concentration. When the ionic strength is increased the double layer width will decrease and hence the overall capacitance (permittivity) also tends to increase. But, at the same time opposing to this effect there is a decrease in the overall sensor permittivity up on increasing ionic strength due to the replacement of water molecules with salt molecules of lower dielectric constants.

In order to monitor the formation of the bio-recognition layer, measurements were taken before and after probe immobilization. After immobilization, a solution of complementary oligomers (5'-CTG CTA CGT G-3') of concentration varying from

0.1μM to 1μM was added on the sensor surface and left to interact over a short period of time. After a short incubation time, the variation of the dielectric spectrum was recorded.

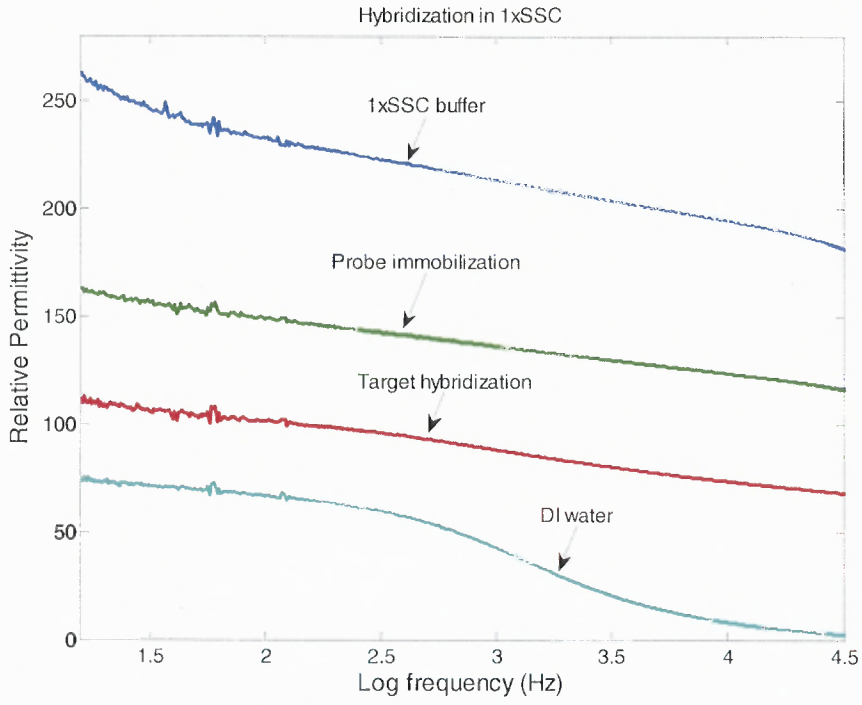


**Figure 3.12** The dielectric spectrum after probe immobilization and target oligomer hybridization. The replacement of water molecules (ε= 80) by oligonucleotide sequences of lower dielectric permittivity is reflected as a decrease in the overall sensor permittivity.

To monitor the exact response of the sensor towards the hybridized targets, the measurement was taken after the removal of nonspecifically bound targets by washing. The relative permittivity changes after single stranded probe oligomer immobilization and target hybridization is shown in Figure 3.12.

The immobilization of oligomer probes decreases the sensor permittivity which can be explained by the replacement of water molecules of high relative permittivity

biomolecules of low relative permittivity. The hybridization of complimentary target sequences to the immobilized probe sequences further enhances this effect. Figure 3.13 shows the dielectric spectrum after the interaction of the immobilized probe sequences to the sample of non-complimentary target sequences.

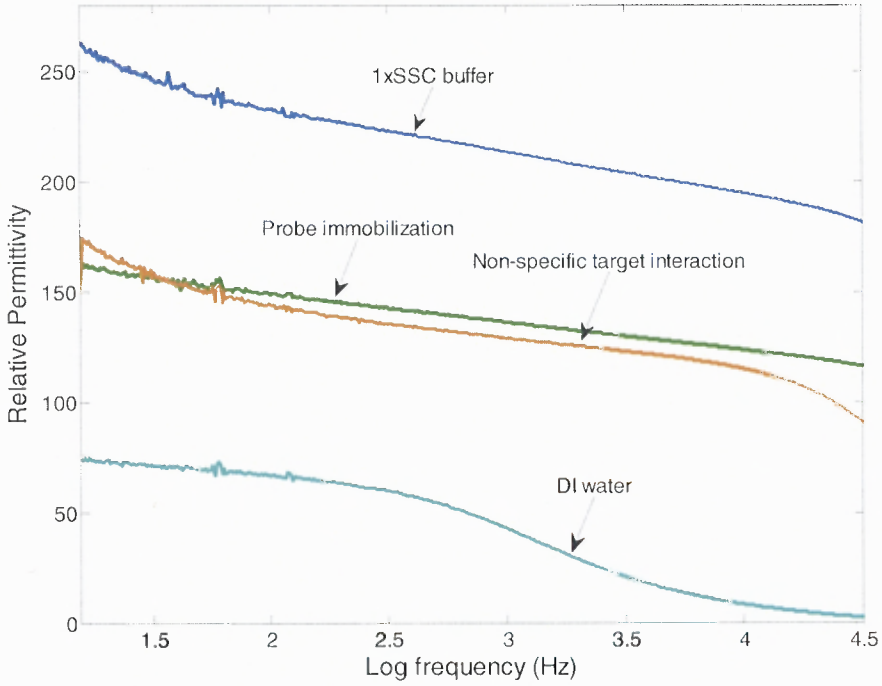


**Figure 3.13** Dielectric Spectra after the interaction of non-complementary target with the immobilized probe sequence. The slight variation in relative permittivity value indicates the non-specifically bound oligomers.

Only negligible change in dielectric property is observed upon the exposure to the non complementary sequence. This supports the relationship between capacitance change and specific nucleotide interaction.

# CHAPTER 4

# FIELD EFFECT CAPACITIVE SENSORS FOR REAL-TIME MONITORING OF NUCLEIC ACID INTERACTIONS

Field effect based devices which utilizes the intrinsic negative charge of the Nucleic Acid molecules for the generation of a sensing signal represent a second set of biosensing architectures of great potential interest. The compatibility of these devices with the standard micro and nano fabrication techniques makes them cost-effective. This class of sensors operates by the field effect modulation of charge carries in a semi conductive region, due to the presence of charged analyte biomolcules. The adsorption or binding of charged macromolecules such as DNA and protein on to the gate electrode of these device structures will effectively alter the surface potential at the gate/electrolyte interface, which in turn produces a redistribution of charge carriers in the semi conducting (Si) region of the sensor. Therefore In the recent years several experimental attempts have been made for the label free detection of biomolecular interactions using by their intrinsic molecular charge using various configurations of Field effect based sensing devices. Ion sensitive Field effect transistor (ISFETs) and its relatives (Enzyme FETs BioFETs) and Capacitive Electrolyte-Insulator Semiconductor structures (EIS) represent two major examples of the Field effect device architectures [8, 54-64].

## 4.1 Field Effect Transistor (FET) based Sensors

Most of the successful research works in this direction have made use of a Field Effect Transistor (FET) structure [62]. The physical structure of a FET type biosensor for detecting DNA and protein molecules is very similar to the MOSFET structure and hence

the operating principle can be explained based on the MOSFET operation theory. The presence of charged macromolecules as a result of immobilization will modify the distribution of charge carriers in the channel region of the semiconductor and these changes will be visible in the I-V characteristics of the device. The addition of charged macromolecules as a result of hybridization or other biomolecular interaction will enhance this effect. Ion Sensitive Field Effect Transistor (ISFET) sensors consists of a MOSFET structure with the gate electrode replaced by an ion sensitive membrane, analyte solution and a reference electrode.

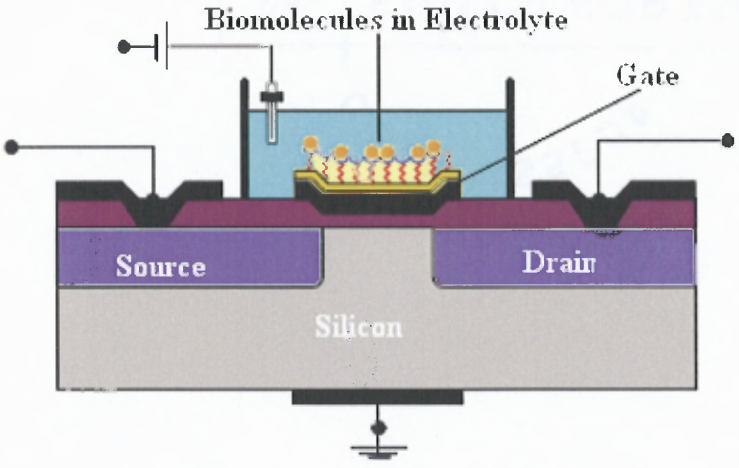


**Figure 4.1** Schematics of a Field Effect Transistor (FET) based biosensor.

The selectivity and chemical sensitivity of the ISFET structure depends on the electrochemical properties of the insulator/electrolyte interface. FET structures with different gate insulator materials such as SiO2, SiO2-Si3N4, silanized SiO2, SiO2 –poly lysine, Al2O3, Ta2O5 etc. with varying thickness between a couple of nanometers to microns have been reported in the literature for biomolecular detection and pH sensing.

Many affinity based biosensor have been developed by the immobilization of the specific probe molecules on the gate material using the appropriate linking chemistries.

In this work the potential of a simple and easy to fabricate Metal Oxide Semiconductor (MOS) capacitive structure in providing real-time monitoring and sensitive detection of oligonucleotide hybridization is demonstrated. The experiments performed show that there is almost no advantage in using a MOSFET (Metal Oxide Semiconductor Field Effect Transistor) structure to obtain the information equally accessible with a MOS capacitor, which is much easier to fabricate and analyze. In particular, the simultaneous shift in the C-V characteristics of a MOS capacitive sensor along both the capacitance and voltage axis makes the C-V method more informative than a static DC measurement on the transistor structure.

## 4.2 MOS Capacitor Operation

MOS capacitive structures have been used as a powerful diagnostic tool in both monitoring integrated circuit fabrication and studying the electrical properties of the MOS field effect system, because of its simplicity in fabrication and analysis [65].The Field Effect Principle owes its origin to Liandrat G, who proposed in 1935 that the conductivity of a semiconductor material can be modified by the application of an external electric field [66].

Considering an nMOS system (p-Si) the application of a negative potential on the gate metal (Au), will accumulate the majority carriers (holes) underneath the gate dielectric (SiO2) thus forming an accumulation region. Upon increasing the voltage to the positive side, the majority carriers will be repelled away from the area beneath the gate

dielectric leaving behind negative ions resulting in the depletion region. The number of these ions equals the number of positive charges on the gate to preserve electrical neutrality. Further increment of voltage results in a higher number of charges on the gate electrode than the number of ions in Silicon. This leads to the appearance of negative mobile carriers- electrons, near the interface region of greatest voltage forming the inversion layer.

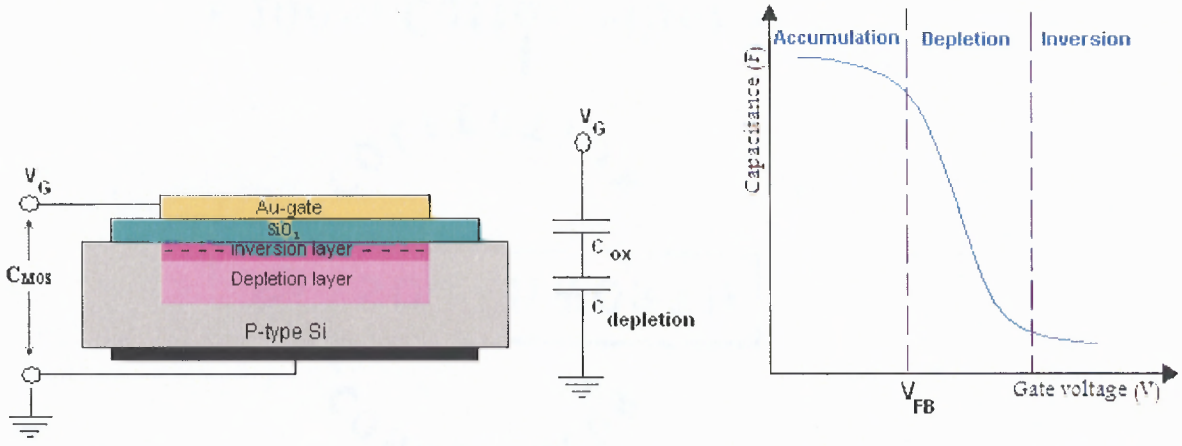


**Figure 4.2** (a) Schematic representation of a Metal-Oxide-Semiconductor Capacitive Sensor operation. (b) Capacitance-Voltage Characteristics (C-V) of an nMOS system (p-type Si) showing accumulation, depletion and inversion regions of operation.

These changes can be monitored by measuring the capacitance across the MOS structure as a function of gate bias VG. For measuring this C-V characteristic a DC polarization voltage is applied on the gate metal (Au) to set the working point of the sensor and a small superimposed (100mV) AC signal is applied to measure the capacitance of the device. The depletion region of the C-V curve is found to be more useful for biosensing applications.

### 4.3 Bio-molecular Sensing Principle

During the immobilization of DNA molecules, the intrinsic negative charge due to the phosphate backbone will effectively alter the surface potential at the gate metal (Au) which induces a change in charge distribution in the silicon underneath as described above. The presence of an additional charged molecular layer due to hybridization enhances the effect. These charge redistribution in silicon layer due to the presence of biomolecules modifies the depletion capacitance ($C_{depletion}$) and is reflected as a shift along the capacitance axis of the C-V characteristics. The C-V characteristics will also be shifted along the voltage axis of due to the interfacial potential difference at the Au/sample interface resulting from biomolecular interactions, which is in series with the applied gate voltage $V_G$. The immobilization and hybridization event can be electrically modeled as the transfer of a certain quantity of charge from the solution to the gate metal (Au).

Equivalent circuit of a MOS capacitor can be simplified as a series connection of voltage independent oxide capacitance $C_{ox,}$ and voltage dependent space charge capacitance of the Si, $C_{Si}$ which gets modified with the electrolyte/metal (Au) interface potential ϕ.

$$C_{MOS} = \frac{c_{si} \times c_{ox}}{c_{si} + c_{ox}} \tag{3.1}$$

In literature, Field effect devices with different sensor configurations have been described; Transistor structures without having an immobilized probe layer had the disadvantage of reduced charge effects due to molecular interactions happening outside

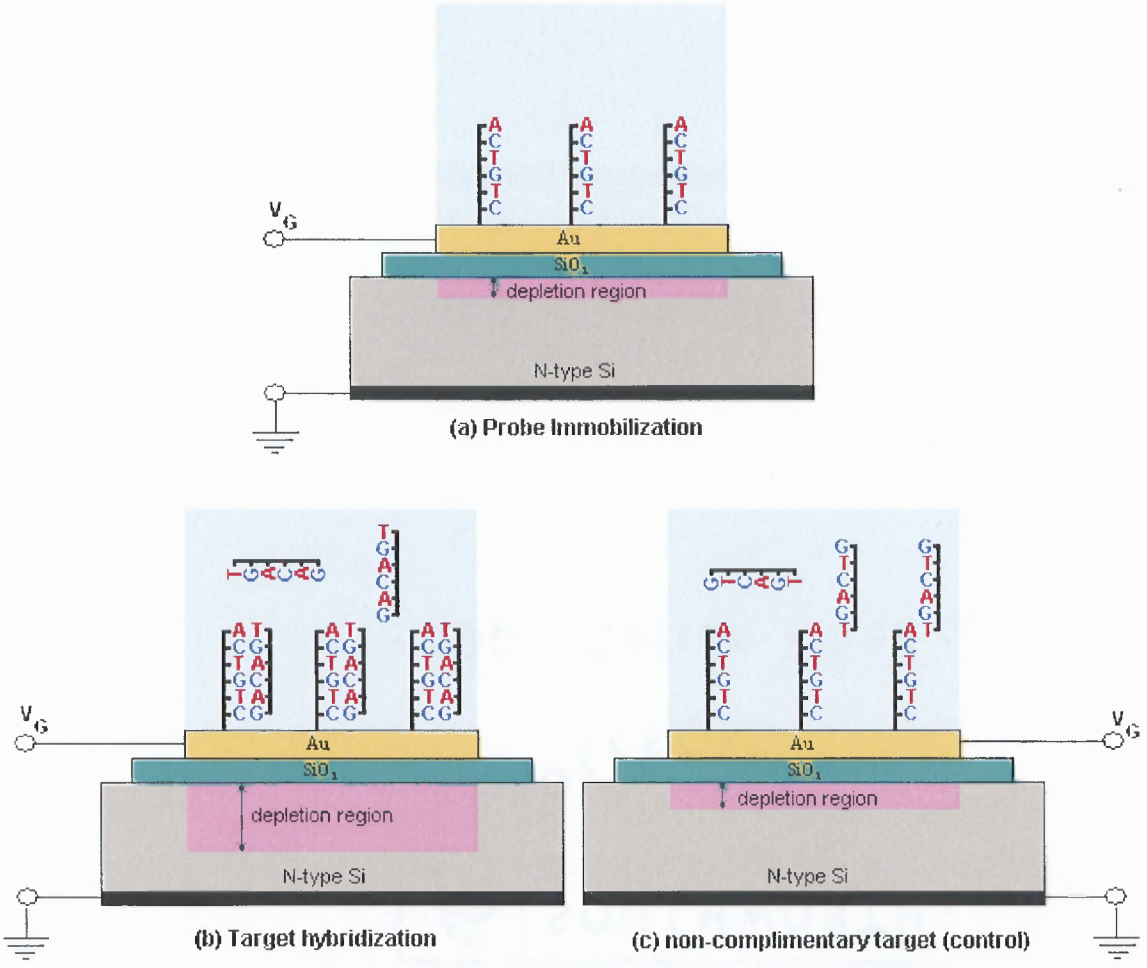


**Figure 4.3.** Schematic showing the biosensing principle of the Field Effect Sensing devices. The immobilization of the negatively charged single stranded probe oligomers on to the gate surface (Au) extends the depletion region in the Silicon (a). Hybridization of the complimentary target sequences to the immobilized probe sequences further increases the depth of the depletion region in Si (b). Exposure of the bio-functionalized sensor to non-complimentary target sequences produces negligible change in the depth of the depletion region (c).

the Debye Layer. The screening of molecular charges due to counter ions reduces the sensitivity towards the biomolecular interactions. Similar is the case with capacitive structures based on an Electrolyte-Insulator-Silicon structure with probe sequences immobilized on biomimetic surfaces like polylysine [8] or agarose [67]which has a fraction of DNA charge above the detectable region due to increased thickness of the

biomimetic layers. Although, the above problem has been solved by tethering the molecules directly on to the gate insulator [68] ($SiO_2$,$Si_3N_4$) surfaces contamination/uncontrolled modifications of these materials in contact with the electrolyte solution possesses a significant problem to the reproducibility of the measurements. The use of a thin film of gold as the gate material in our sensing structure offers several advantages. The chemical inertness of gold protects it from getting oxidized by the electrolytic environment. Moreover, the chemistry of covalent immobilization of probe sequences using alkyl thiol linkage has been well studied and the immobilization is easily achievable.

## 4.4 Sensor Fabrication and Measurement setup

The MOS capacitive sensors used in this work were fabricated on n-type Silicon wafer with resistivity 10 ohm-cm. A thermal oxide layer of <10 nm is grown as the gate insulator. The sensitivity towards gate surface potential changes is enhanced by the use of this extremely thin layer of gate insulator [69]. Circular regions of 150nm thick, 2mm diameter gold regions are deposited as the gate electrode. A 10nm Titanium layer is used to promote the adhesion of gold to $SiO_2$. Back side Ohmic contact is provided by a 150nm layer of Al on silicon. The performance of the MOS capacitive sensors in monitoring biomolecular interactions were studied by analyzing Capacitance-Voltage (C-V) characteristics across the device.

The C-V characteristics were analyzed in a probe station using HP4145B Semiconductor Parameter Analyzer. Capacitance-Voltage (C-V) curves were obtained by varying the gate voltage from 1.5V (accumulation) to -1.5V (inversion) through the

depletion region (0.5 to -0.7 V).The effect of electric field in enhancing the immobilization density, rate of hybridization and selectivity towards target sequences were investigated by applying sufficient potential to the gate metal.

Materials

DNA oligonucleotides including the thiol labeled probe sequences used for the experiments were purchased from IDT (Integrated DNA Technologies). 20xSSC buffer solution (3.0M Sodium Chloride + 0.3M Sodium Citrate) used for the hybridization assay was purchased from Sigma-Aldrich. The chemicals and other materials used for microfabrication of the device were obtained from Microfabrication Center at New Jersey Institute of Technology.

### 4.5 Probe Immobilization and Target Hybridization Procedure

Single stranded DNA sequences pre-modified by the thio linker (5'-CACGTAGCAG/3Thio MC3-D/-3') were immobilized on the gold metal gate using a concentration of 10uM in 0.05xSSC buffer. By taking advantage the high affinity of sulphur atoms to gold substrate the DNA molecules with thiol end groups are chemically assembled onto the gold surface from the solution [50, 51]. The oligomer chains are thus tethered to the gold substrate at one end and the rest of the chain stays fully extended at an angle of approximately 30 degree from the surface. The Van der Waals forces between adjacent chains helps to order the oligomers parallel to each other [52]. The <111> crystal orientation of gold which is obtained by thin film deposition of gold on SiO2 is found to give excellent result for the formation of self assembled monolayers (SAM)[53]. Mercapto hexanol (HS- (CH2)6 OH ) SAM layers were immobilized in between the

DNA strands in order to passivate the vacant spaces. Mercaptohexanol layer would also help in providing an upright position for the oligomers due to electrostatic repulsion. Prior to immobilization procedure the structure was cleansed using acetone, isopropanol and deionized water.

## 4.6 Results and Discussion

The Capacitance-Voltage characteristics for the bio-fuctionalization procedure were monitored in real-time. Figure 4.4 shows the C-V characteristics at various time intervals of the MOS capacitive sensor before and after the oligomer probe introduction. The constant shift of the characteristics to the side of positive gate voltage confirms the presence of more negative charge on the gate surface. A shift of 140 mV is observed due to immobilization after the exposure of the gold electrode to the thiol labeled probe sequences for 25 minutes. The substrates with immobilized oligomers were then allowed to interact with 1μM concentration of complementary oligomers (5'-CTG CTA CGT G-3') over a short period of time. Figure 4.4 shows the C-V characteristics of the MOS structure during hybridization event at various time intervals. Due to the hybridization of the complimentary sequences a further shift of 73 mV towards the positive side is observed after 20 minutes. This agrees with the presence of an additional layer negatively charged DNA molecules.

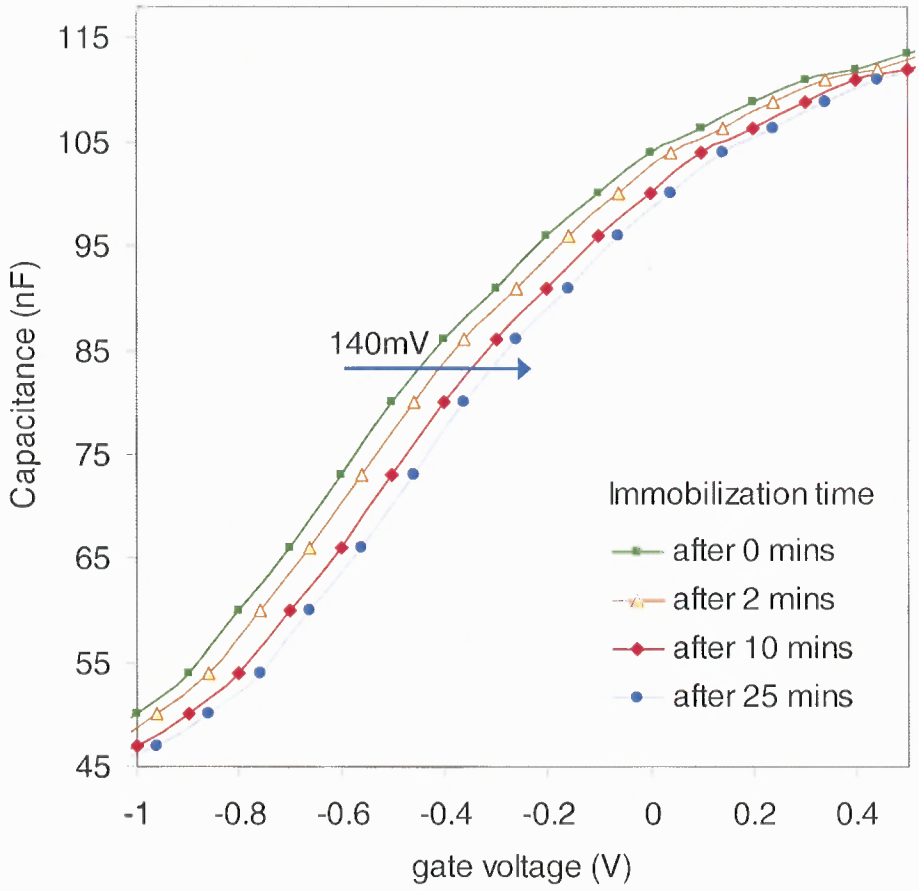


**Figure 4.4.** Capacitance-Voltage characteristics measured at various time intervals during the immobilization of single stranded probe DNA sequences. A positive shift in the characteristics can be observed as a result of the immobilization of negatively charged oligonucleotide molecules.

As a control experiment, non-complementary target sequences (5'-ATG GCC CTG T-3') of same concentration as the complementary target solution is allowed to interact with the immobilized probe layer. Figure 4.6 shows negligible change in dielectric property upon exposure to the non complementary sequence for a time period of 25 mins. This supports the relationship between capacitance change and specific nucleotide interaction.

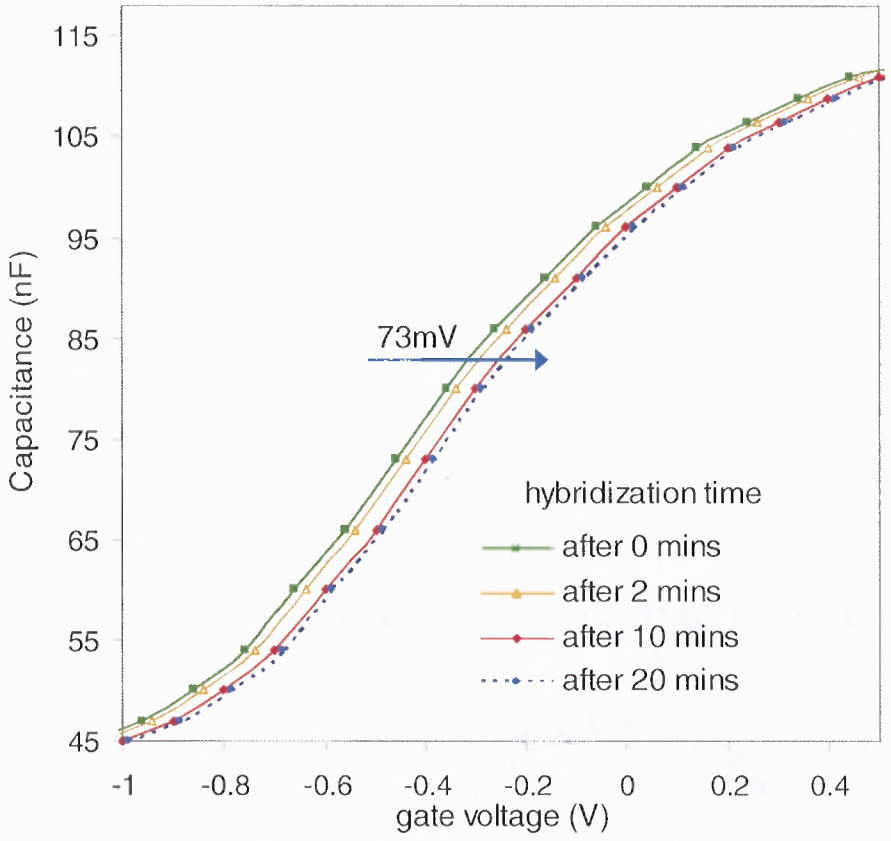


**Figure 4.5.** Capacitance-Voltage characteristics measured in real-time during the hybridization of immobilized probe sequences with complimentary target sequences. The binding of DNA molecules results in a further positive shift in the C-V characteristics due to their intrinsic negative charge.

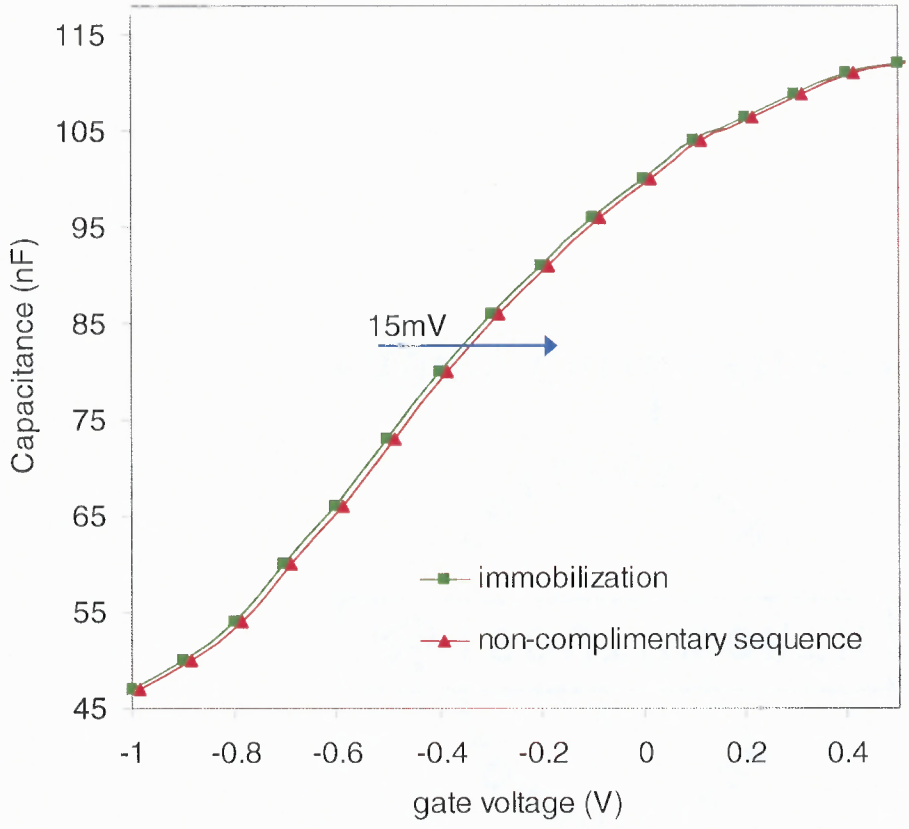


**Figure 4.6** C-V characteristics as a result of the interaction of immobilized probe sequences with non-complimentary targets.

## 4.7 Conclusions of the Study

In this study, the use of Metal-Oxide-Semiconductor (MOS) Field Effect Capacitive sensors in providing label-free, real-time monitoring of oligonucleotide hybridization is demonstrated. The immobilization of probe oligomers on the sensor surface and their hybridization with the target oligomers of complimentary sequences has produced a significant shift (140mV and 73mV respectively) in the Capacitance-Voltage characteristics measured across the device. The active area of the sensor can be further

miniaturized using standard photolithographic techniques promoting massively parallel screening of nucleic acid samples in array formats.

## 4.8 Dual Parametric Capacitive Sensors

In an attempt to utilize the individual merits of nanoscale electrochemical capacitive sensor and field effect MOS capacitive structure, a novel dual parametric sensing architecture encompassing both these transducing elements on a single sensor is proposed. The nano-scale Debye capacitive element consisting of gold electrodes measures and detects the **Dielectric permittivity (ε)** changes up on analyte-probe interactions, while the Field effect capacitive element monitors and detects the **Surface potential (ψ)** changes up on the binding of the charged biomolecules. The detection scheme based on the combined analysis of the two parameters- Dielectric property and intrinsic molecular charge- of biomolecules has found to reveal complimentary information of significance about the analyte-probe interactions.

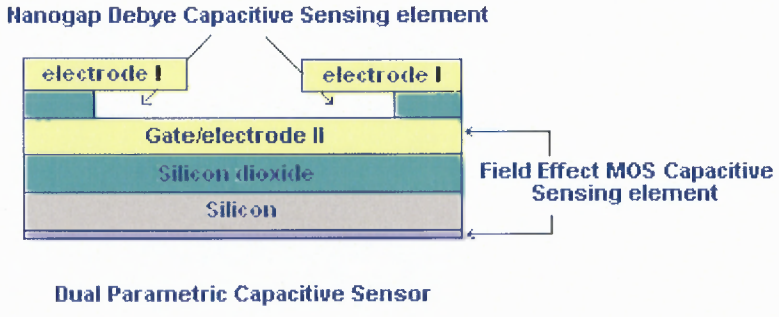


**Figure 4.7** Schematics of a Dual Parametric Capacitive sensor comprising of both the nano-scale capacitive sensor and the Field effect capacitive sensor on a single device architecture.

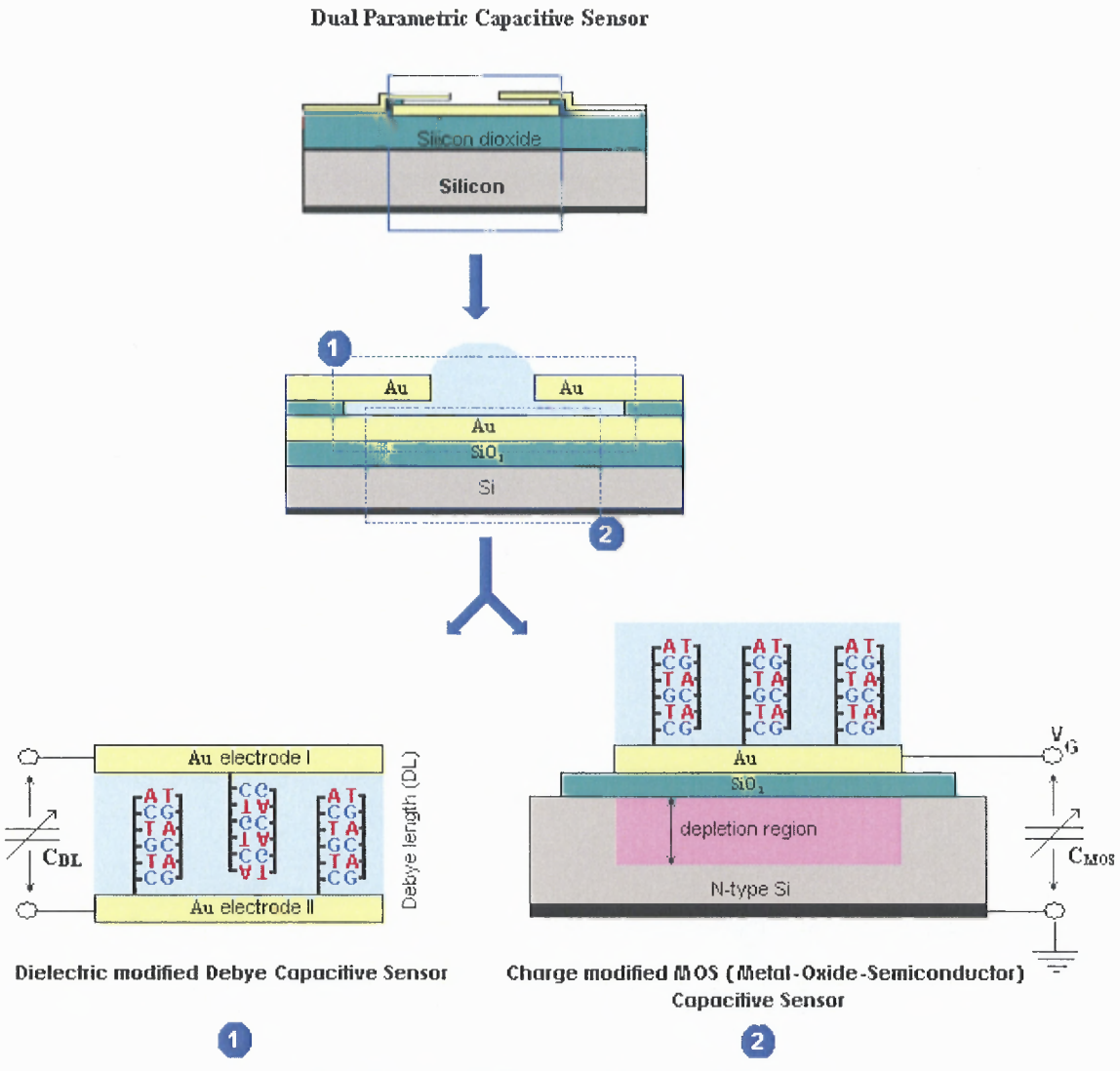


**Figure 4.8** Operating principle of the dual parametric capacitive sensor.

# CHAPTER 5

# ELECTRIC FIELD ASSISTED IMMOBILIZATION, HYBRIDIZATION AND IMPROVEMENT IN SELECTIVITY- ACTIVE SENSING MECHANISMS

## 5.1 Introduction

The last two chapters have presented two promising biosensig device architectures and demonstrated their advantages over the already developed techniques. These sensing mechanisms with their improved sensitivity and the use of reduced sample volume gives promises for serving as building blocks of point of care diagnostics or other such portable hand-held diagnostic tools. Generally the DNA hybridization experiments utilizing any such sensing mechanisms are carried out under conditions where the reaction rates and selectivity (stringency) conditions are controlled by varying target NA concentration, temperature, or ionic strength of the buffer solution used. Although such classical, passive hybridization assay procedures utilizing optical detection mechanisms are already developed, such approaches limit the degree to which the detection speed and specificity or selectivity can be improved. By the development active sensing mechanisms utilizing precisely controlled electric fields, the rate and the selectivity of the detection process is demonstrated to be immensely improved.

## 5.2 Active Sensing Principle

Since oligomers in solution carry a net negative charge, they can be transported towards the probe molecules immobilized on the sensor surface (Au) by applying a positive bias on the surface. Such electrophoretic transport of the thiol labeled oligomer probe molecules enables the functionalization of the sensor surfaces selectively at a much faster

rate than the passive immobilization techniques. The application of electric field of appropriate polarity and controlled intensity can also help in improving the hybridization rate and efficiency. The electric field will help offset the electrostatic repulsion between the negative charges on the immobilized probe and target molecules in solution [70]. The orientation of the Probe oligomers immobilized on the sensor surface can also be controlled by the applied electric field [71].

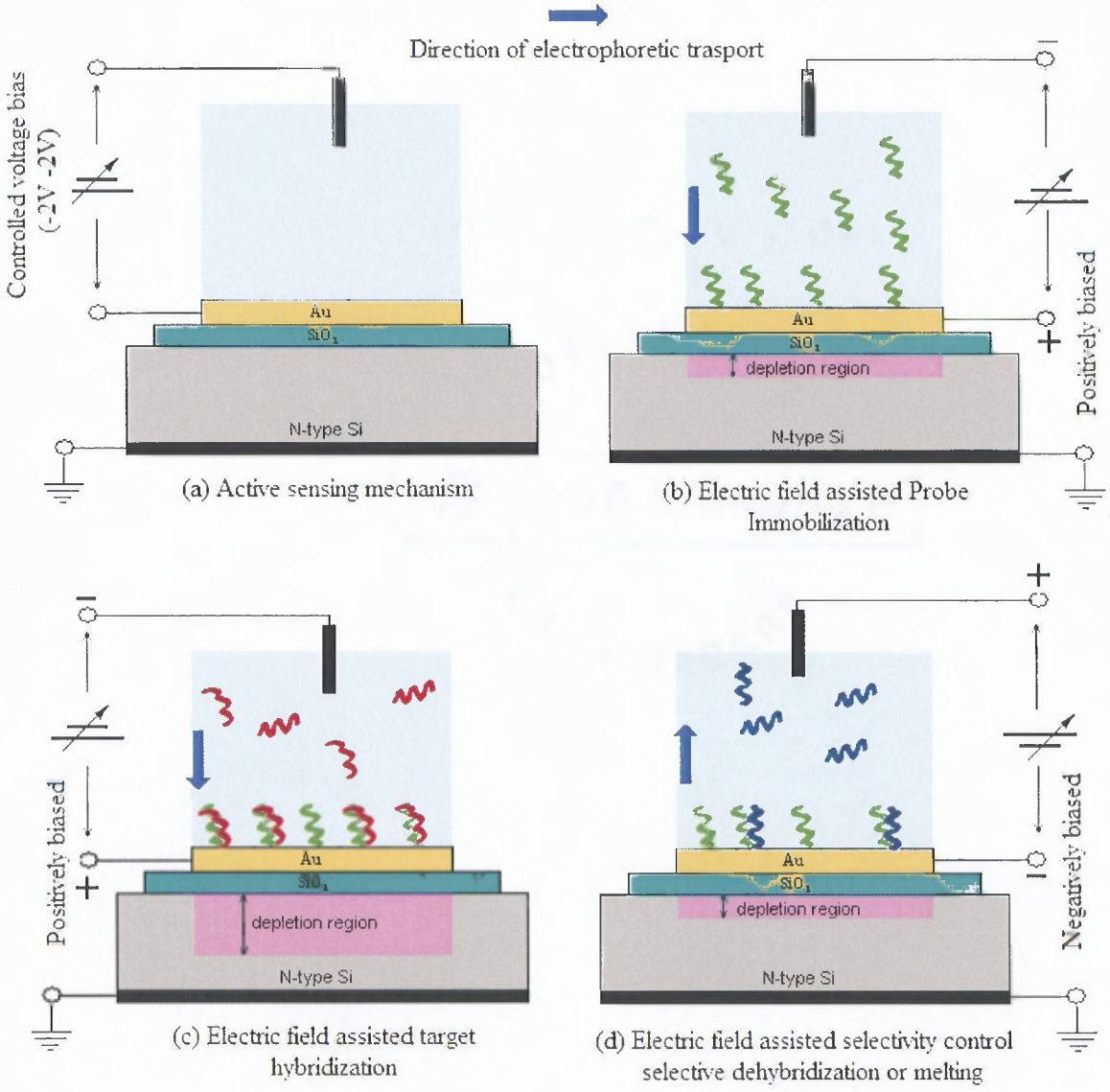


**Figure 5.1** Schematic representation of an active sensing mechanism based on MOS capacitive sensors.

This electric field assisted transport of oligomers towards the immobilized probes will not only compensate for the reduced ionic strength but also enhance the rate of hybridization. The movement of the target nucleotide molecules toward the immobilized probe sequences, facilitated by electric field can result in a concentrating effect of the target molecules near the surface. This can result in the binding of probe and target sequences in a much higher rate.

The electric field induced (electrophoretic) transport of nucleotide molecules can be also used for enhancing the selectivity of the sensing process. The selectivity of the sensing process depends on the specificity of the binding between the target and probe sequences. The unhybridized target molecules which stay non-specifically bound on the sensor surface will also contribute to the sensing signal. By applying a negative bias on the Gold (Au) surface these non-specifically bound target nucleotide molecules can be released and repelled away from the sensing area, thereby eliminating their effect on the sensing signal.

By adjusting the electric field to the appropriate level, selective dehybridization (melting) of the target-probe pair depending up on their degree of complimentarity is also made possible. Analyzing the melting curves of various target-probe pairs as a function of the bias voltage (V) will provide much more information to differentiate between closely related targets sequences. Such techniques are promising for applications such are single nucleotide polymorphism (SNP) analysis.

Nanogen has initially developed the concept of electric field assisted DNA immobilization [70, 72-75] with the intension of increasing the hybridization rates on the chip and providing improved immobilization selectivity. The DNA chip (NanoChip$^{TM}$)

developed by Nanogen utilizes the controlled electrophoretic transport of the DNA molecules to achieve pixel to pixel selectivity in the probe immobilization procedures.

## 5.3 Experimental Methods

A systematic study of the effect of external electric field on the immobilization of single stranded probe sequences and their hybridization with the target sequences utilizing a Field effect capacitive sensing mechanism has been conducted. The use of precisely controlled electric field of appropriate polarity to improve the selectivity of the detection process through the attainment of selective melting of the partially hybridized target-probe pairs has also been demonstrated. In our experiments, the Metal Oxide Semiconductor, (MOS) field effect capacitive sensor described in Chapter 3 is used as the detection device due to the easiness of sample handling and measurement setup compared to the nano-cavity capacitive sensors. As a first step the electric field is applied during the NA immobilization process. Initially, a voltage varying from 0 to 5V was applied between the Aluminum back contact and a Pt wire immersed in the sample solution with the Si back contact positively biased. A problem associated with applying the voltage through the Si back contact (Al) most of the applied potential is dropped across the Silicon dioxide layer. Since the capacitance of the dioxide layer is much smaller (60nF $cm^{-2}$) than the double layer capacitance value observed for Au (3 $\mu F\ cm^{-2}$) only a small fraction of the applied potential will fall in the double layer of bare gold surface. Hence only approximately 1/500 of the applied voltage will have an effect in promoting the immobilization or hybridization events. In order avoid this situation in the later set of experiments the voltage was applied directly to the gold gate surface of the MOS

capacitor with respect to the Pt electrode in contact with the solution. The Aluminum back contact of the Silicon substrate was kept grounded during the field assisted immobilization and hybridization procedures.

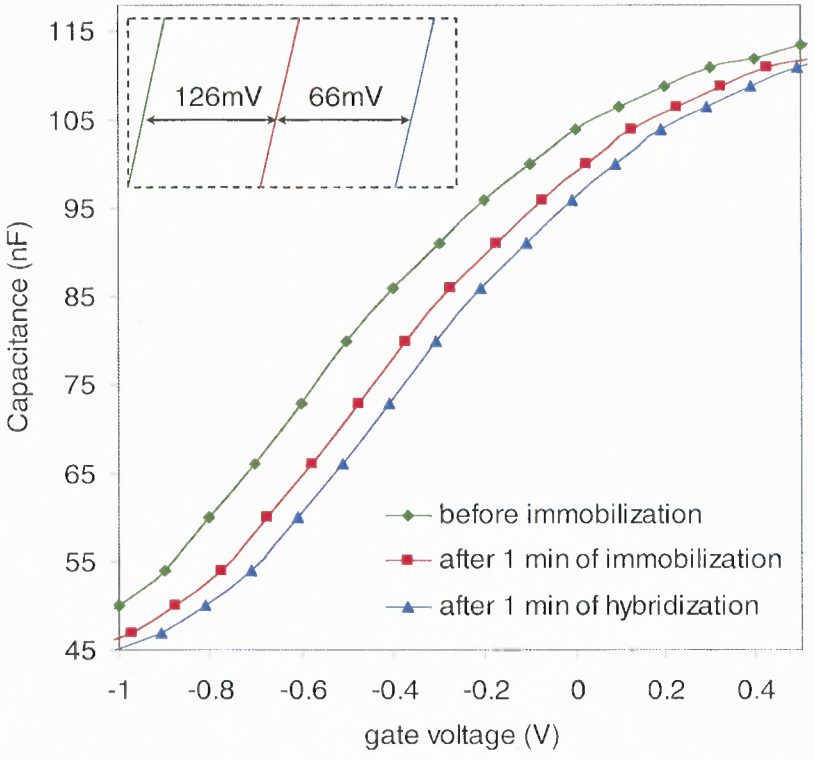


**Figure 5.2** C-V characteristics of the Field Effect Capacitive sensor after 60s of electric Field assisted immobilization and hybridization procedures.

The immobilization experiments has been done with probe oligomer sequences pre-modified by the thio linker (5'-CACGTAGCAG/3Thio MC3-D/-3') with a concentration of 10μM in 0.05xSSC buffer under the effect of 0.3 to 0.7 V applied between the Gold gate electrode and the Pt electrode immersed in the sample solution. Figure 5.2 shows the results for the field assisted immobilization and hybridization procedure. The electric field assisted transport of thiol-labeled probe oligomers towards the Au surface resulted in the attainment of immobilization at a much faster rate. A positive shift of 126 mV is

observed after the exposure of sensor surface to the probe molecules for 1 min, under the presence of electric field. Increasing of the voltage range above 1 V caused the gold thin film to peel off from the sensor surface.

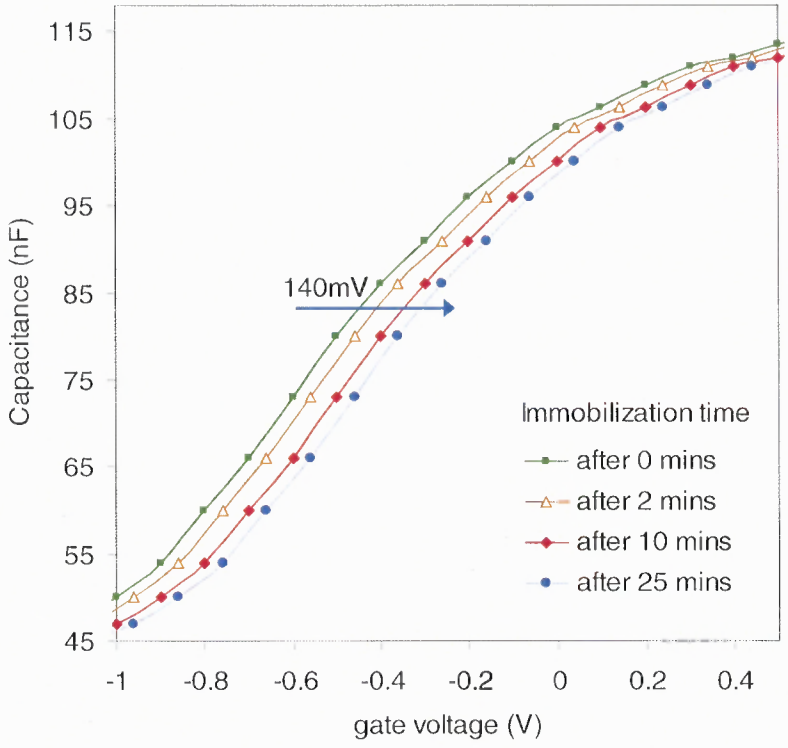


**Figure 5.3** Capacitance-Voltage characteristics measured at various time intervals during the immobilization of single stranded probe DNA sequences. A positive shift in the characteristics can be observed as a result of the immobilization of negatively charged oligonucleotide molecules.

Under normal conditions, immobilization of probe molecules on to Gold electrodes utilizing thiol linkages takes 20-25 minutes to attain a the similar variation in the measured C-V characteristics. For the ease of comparison the results obtained during the immobilization procedures without the effect of electric field is also shown below in Figure 5.3. The effect of an electric field on the hybridization procedures using complimentary target sequences was also studied. The substrates with the immobilized

oligomers were then allowed to interact with 1μM concentration of complementary oligomers (5'-CTG CTA CGT G-3') for a time period of 1 minute under the influence of 0.3 V- 0.7 V applied to the gate electrode with reference to the Pt electrode.

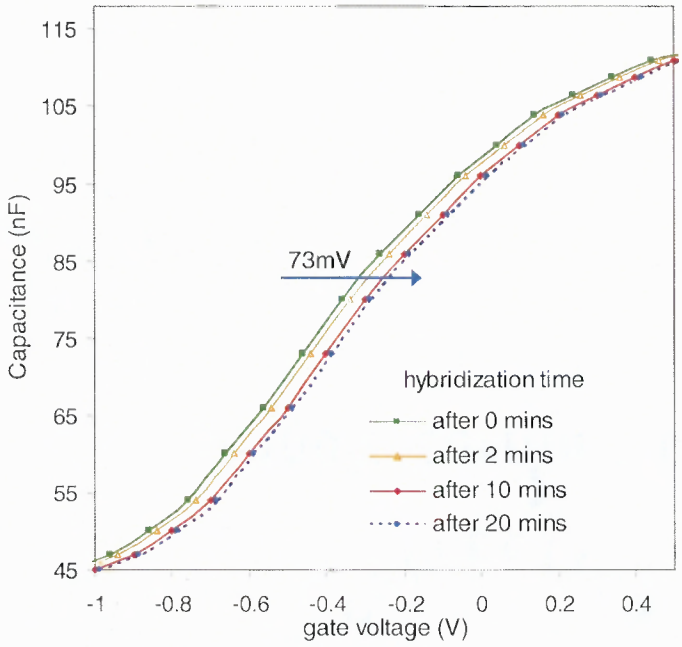


**Figure 5.4** Capacitance-Voltage characteristics measured in real-time during the hybridization of immobilized probe sequences with complimentary target sequences. The binding of DNA molecules results in a further positive shift in the C-V characteristics due to their intrinsic negative charge.

The localized concentrating effect of the target molecules near the immobilized probe surface resulted from the field assisted transport enabled the binding of probe and target sequences at a much higher rate. From Figure 5.2 a positive shift of about 66 mV is observed after interaction of probe molecules with the complimentary target sequences for 1 minute. The C-V characteristics obtained during normal hybridization procedures without the effect of electric field is also shown below in Figure 5.4 for comparison. Under normal conditions 20 minutes of interactions between the immobilized probe sequences and the probe molecules resulted in a shift of 73 mV in the C-V characteristics.

These results confirm that under the influence of electric field both the immobilization and hybridization processes are strongly promoted and the efficiency is much higher. The application of electric field could be also used to enhance the selectivity of the molecular detection process.

## 5.4 Active Sensing, Advantages and Applications

The active electronic sensing mechanism proved to be feasible on field effect capacitive devices can be extended to sensing array formats. The electrophoretic fields produced due to the application of appropriate current and voltage levels to such sensor arrays can be used to transport and concentrate nucleic acid molecules on to the specific (positively biased) test sites. By designing the microelectrode array can be designed in such a way that the test sites or the microsensing locations on its surface can be negatively or positively biased in any desired configuration. There fore any desired pattern of nucleic acid transport to one or more than one test location on the array can be attained. Single stranded nucleic acid probes such as oligonucleotides, DNA, RNA, PCR amplicons etc. which are functionalized with thiol labels can be selectively and rapidly transported and bound on to the desired sensing locations.

Similarly, the target nucleic acid sequences in the sample can then be electrophoretically transported, locally concentrated and hybridized on to any specific test sites functionalized with the probe sequences. Heller et al.has demonstrated similar techniques associated with fluorescence based detection mechanism. As clearly observed in the experimental results such rapid transport and associated localized concentrating effect of the target nucleic acid sequences near the sensing areas will lead to a significant

reduction in the hybridization time and hence an immense improvement in the efficiency of such detection mechanism when compared to the passive hybridization assays. This has profound advantages in the development of diagnostic tools without performing prior analyte amplifications such as point of care diagnostic devices. In such real life situations where the concentration of the target DNA is low active electronic technique can be developed to attain hybridization in minutes or even seconds with higher efficiency where as the conventional passive techniques could take hours.

By reversing the electric field bias applied to the sensing area (negative bias), rapid removal of the unhybridized nucleic acid molecules can be achieved. Also, by adjusting the electric field to the appropriate intensity selective dehybridization (melting) of the target anlayte molecules from the immobilized probe sequences depending on their degree of complimentarity can be attained. This novel technique of "electronic stringency control" can serve as a reliable and rapid technique for discriminating single base mismatches in point mutations and Single Nucleotide Polymorphisms (SNPs) [76, 77].

## 5.5 Summary of the Study

The improvement in the detection speed and selectivity by the use of external electric field has also been demonstrated. The immobilization of the single stranded probe sequences was clearly found to be promoted by the external electric field. The application of a positive bias of 0.3 V to 0.5 V during the immobilization procedure created a positive shift of 126 mV with in 1 minute compared to the shift of 140 mV produced by 25 minutes under normal conditions. More importantly, the hybridization of the target sequences was strongly promoted by the external electric field of favorable polarity and

required hybridization efficiency was attained with in 1 minute of exposure to the immobilized probe sequences. Future work will be concentrated on optimizing this technique to be able to discriminate single base pair mismatches and also in developing sensing architectures with higher degree of parallelism. From reports in the literature by Fixe et al. (2003) suggest that the application of fast electric pulses has been used to reduce the hybridization time to the seconds range. The electric field assisted immobilization procedures are promising for applications where different probe sequences are required to be immobilized at specific sites of an array of sensors.

# CHAPTER 6

# SUMMARY & FUTURE DIRECTIONS

## 6.1 Summary of the Study

In this work, two separate sensing mechanisms have been demonstrated for the label-free electrical detection of nucleic acid hybridization. In the first section, capacitive biosensors with electrode separation in the order of electrical double layer width were designed and fabricated using SiO2 sacrificial layer techniques. The nano scale electrode space confinement is shown to eliminate noises from electrode polarization effect and solution conductivity, permitting the dielectric spectroscopic measurements at low frequencies. DNA hybridization experiments with complementary and non complementary target sequences were performed and a 30-40% change in sensor permittivity (capacitance) was observed after the hybridization of the immobilized probe with the complementary oligomer sequences. Work is presently being carried out in order to optimize the detection mechanism and improve the sensitivity and selectivity of the sensor. Ideally, Single Nucleotide Polymorphism (SNP) could be detected with the current geometries of the device. The improved sensitivity demonstrated by the Debye Capacitive sensor combined with its use of reduced sample volume and low fabrication cost makes it promising for applications such as point of care diagnostics and biowarfare agent detection.

In parallel to the above work, the applications and advantages of a Metal-Oxide-Semiconductor (MOS) Field Effect Capacitive sensor in providing label-free, real-time monitoring of oligonucleotide hybridization was demonstrated. The immobilization of probe oligomers on the sensor surface and their hybridization with the target oligomers of

complimentary sequences has produced a significant shift (140mV and 73mV respectively) in the Capacitance-Voltage characteristics measured across the device. The active area of the sensor can be further miniaturized using standard photolithographic techniques promoting massively parallel screening of nucleic acid samples in array formats.

In the final section of the thesis the proof of principle of a novel technique of enhancing the speed and selectivity of the molecular detection processes by the application of an external electric field of appropriate intensity was demonstrated. Future work will be concentrated on optimizing this technique to be able to discriminate single base pair mismatches and to improve the concentration sensitivity of the sensor.

## REFERENCES


1. B. Pejcic, R.D. Marco, and G. Parkinson, "The role of biosensors in the detection of emerging infectious diseases," *Analyst*, vol. 131, no. 10, pp. 1079-1090, 2006.

2. J. Fritz, M.K. Baller, H.P. Lang, H. Rothuizen, P. Vettiger, E. Meyer, H.J. Guì^ntherodt, C. Gerber, and J.K. Gimzewski, "Translating biomolecular recognition into nanomechanics," *Science*, vol. 288, no. 5464, pp. 316-318, 2000.

3. S. Howorka, S. Cheley, and H. Bayley, "Sequence-specific detection of individual DNA strands using engineered nanopores," *Nature Biotechnology*, vol. 19, no. 7, pp. 636-639, 2001.

4. B.P. Nelson, T.E. Grimsrud, M.R. Liles, R.M. Goodman, and R.M. Corn, "Surface plasmon resonance imaging measurements of DNA and RNA hybridization adsorption onto DNA microarrays," *Analytical Chemistry*, vol. 73, no. 1, pp. 1-7, 2001.

5. Y. Okahata, M. Kawase, K. Niikura, F. Ohtake, H. Furusawa, and Y. Ebara, "Kinetic Measurements of DNA Hybridization on an Oligonucleotide-Immobilized 27-MHz Quartz Crystal Microbalance," *Analytical Chemistry*, vol. 70, no. 7, pp. 1288-1291, 1998.

6. F.C. Tenover, "Diagnostic deoxyribonucleic acid probes for infectious diseases," *Clinical Microbiology Reviews*, vol. 1, no. 1, pp. 82-101, 1988.

7. S.K. Moore, "Making chips to probe genes," *IEEE Spectrum*, vol. 38, no. 3, pp. 54-60, 2001.

8. J. Fritz, E.B. Cooper, S. Gaudet, P.K. Sorger, and S.R. Manalis, "Electronic detection of DNA by its intrinsic molecular charge," *Proceedings of the National Academy of Sciences of the United States of America*, vol. 99, no. 22, pp. 14142-14146, 2002.

9. J.P. Golden and F.S. Ligler, "A comparison of imaging methods for use in an array biosensor," *Biosensors and Bioelectronics*, vol. 17, no. 9, pp. 719-725, 2002.

10. M. Schaferling and S. Nagl, "Optical technologies for the read out and quality control of DNA and protein microarrays," *Analytical and Bioanalytical Chemistry*, vol. 385, no. 3, pp. 500-517, 2006.

11. J.S. Daniels and N. Pourmand, "Label-free impedance biosensors: Opportunities and challenges," *Electroanalysis*, vol. 19, no. 12, pp. 1239-1257, 2007.

12. P. Estrela, A.G. Stewart, F. Yan, and P. Migliorato, "Field effect detection of biomolecular interactions," *Electrochimica Acta*, vol. 50, no. 25-26 SPEC. ISS., pp. 4995-5000, 2005.

13. P. SklaÌ□dal, "Advances in Electrochemical Immunosensors," *Electroanalysis*, vol. 9, no. 10, pp. 737-745, 1997.

14. M. Lohndorf, U. Schlecht, T.M.A. Gronewold, A. Malave, and M. Tewes, "Microfabricated high-performance microwave impedance biosensors for detection of aptamer-protein interactions," *Applied Physics Letters*, vol. 87, no. 24, pp. 1-3, 2005.

15. Y.D. Feldman, Y.F. Zuev, E.A. Polygalov, and V.D. Fedotov, "Time domain dielectric spectroscopy. A new effective tool for physical chemistry investigation," *Colloid & Polymer Science*, vol. 270, no. 8, pp. 768-780, 1992.

16. E.H. Grant, R.J. Sheppard, and G.P. South*Dielectric Behaviour of Biological Molecules in Solution*, 1978.

17. J.B. Hasted*Aqueous Dielectrics*, 1973.

18. S. Takashima*Electrical Properties of Biopolymers and Membranes*, 1989.

19. J. Baker-Jarvis, C.A. Jones, and B. Riddle, "Electrical properties and dielectric relaxtion of DNA in solution," *NIST Technical Note*, pp. 1509, 1998.

20. P.M. Biesheuvel, "Implications of the charge regulation model for the interaction of hydrophilic surfaces in water," *Langmuir*, vol. 17, no. 12, pp. 3553-3556, 2001.

21. M. Mandel, "Dielectric properties of charged linear macromolecules with particular reference to DNA," *Annals of the New York Academy of Sciences*, vol. Vol.303, pp. 74-87, 1977.

22. B. Saif, R.K. Mohr, C.J. Montrose, and T.A. Litovitz, "On the mechanism of dielectric relaxation in aqueous DNA solutions," *Biopolymers*, vol. 31, no. 10, pp. 1171-1180, 1991.

23. S. Takashima, "Dielectric dispersion of DNA," *J. Mol. Biol.*, vol. 7, pp. 455-467, 1963.

24. S. Takashima, "Dielectric dispersion of deoxyribonucleic acid. II," *The Journal of physical chemistry*, vol. 70, no. 5, pp. 1372-1380, 1966.

25. S. Takashima, "Effect of ions on the dielectric relaxation of DNA," *Biopolymers - Peptide Science Section*, vol. 5, no. 10, pp. 899-913, 1967.

26. F. Van Der Touw and M. Mandel, "Dielectric increment and dielectric dispersion of solutions containing simple charged linear macromolecules. I. Theory," *Biophysical Chemistry*, vol. 2, no. 3, pp. 218-230, 1974.

27. C. Chassagne, D. Bedeaux, J.P.M. Van Der Ploeg, and G.J.M. Koper, "Theory of electrode polarization: Application to parallel plate cell dielectric spectroscopy

experiments," *Colloids and Surfaces A: Physicochemical and Engineering Aspects*, vol. 210, no. 2-3, pp. 137-145, 2002.

28. P.A. Cirkel, J.P.M. Van Der Ploeg, and G.J.M. Koper, "Electrode effects in dielectric spectroscopy of colloidal suspensions," *Physica A: Statistical Mechanics and its Applications*, vol. 235, no. 1-2, pp. 269-278, 1997.

29. M. Mandel*Bull. Soc. Chim. Belg.*, vol. 65, pp. 305, 1956.

30. E. Warburg, "Ueber das verhalten sogenannter unpolarisirbarer elektroden gegen wechselstrom," *Ann. Phys. Chem.*, vol. 67, pp. 493-499, 1899.

31. H.P. Schwan and C.D. Ferris, "Four-electrode null techniques for impedance measurement with high resolution," *Review of Scientific Instruments*, vol. 39, no. 4, pp. 481-485, 1968.

32. R. Tamamushi and K. Takahashi, "Instrumental study of electrolytic conductance measurements using four-electrode cells," *Journal of Electroanalytical Chemistry*, vol. 50, no. 2, pp. 277-284, 1974.

33. K.G. Ong, J. Wang, R.S. Singh, L.G. Bachas, and C.A. Grimes, "Monitoring of bacteria growth using a wireless, remote query resonant-circuit sensor: Application to environmental sensing," *Biosensors and Bioelectronics*, vol. 16, no. 4-5, pp. 305-312, 2001.

34. H. Wakamatsu, "A dielectric spectrometer for liquid using the electromagnetic induction method," *Hewlett-Packard Journal*, vol. 48, no. 2, pp. 37-44, 1997.

35. H. Fricke and H.J. Curtis, "The dielectric properties of water-dielectric interphases," *Journal of Physical Chemistry*, vol. 41, no. 5, pp. 729-745, 1937.

36. S. Takashima, "Effect of Ions on the Dielectric Dispersion of Ovalbumin Solution," *J. Polym. Sci. A*, vol. 1, pp. 2791-2803, 1963.

37. M. Mandel and A. Jenard*Bull. Soc. Chim. Belg.*, vol. 67, pp. 575, 1958.

38. T.M. Shaw, "The elimination of errors due to electrode polarization in measurements of the dielectric constants of electrolytes," *The Journal of Chemical Physics*, vol. 10, no. 10, pp. 609-617, 1942.

39. F. Van Der Touw and M. Mandel, "Plane-parallel condenser with variable electrode spacing for determination of electric permittivity of highly conducting liquids below 1 MHz. Part 1. - Theoretical considerations," *Transactions of the Faraday Society*, vol. 67, pp. 1336-1342, 1971.

40. F. Van Der Touw, M. Mandel, D.D. Honijk, and H.G.F. Verhoog, "Plane-parallel condenser with variable electrode-spacing for determination of electric

permittivity of highly conducting liquids below 1 MHz. Part 2. - Experimental approach," *Transactions of the Faraday Society*, vol. 67, pp. 1343-1354, 1971.

41. C.L. Davey, G.H. Markx, and D.B. Kell, "Substitution and spreadsheet methods for analysing dielectric spectra of biological systems," *European Biophysics Journal*, vol. 18, no. 5, pp. 255-265, 1990.

42. J.L. Oncley, "Studies of the dielectric properties of protein solutions. I. Carboxyhemoglobin," *Journal of the American Chemical Society*, vol. 60, no. 5, pp. 1115-1123, 1938.

43. R.J. Hunter*Introduction to Modern Colloid Science*, 1993.

44. R.J. Hunter*Zeta Potential in Colloid Science*, 1981.

45. E.J.W. Verwey, "The electrical double layer and the stability of lyophobic colloids. I. The electrical double layer," *Chemical Reviews*, vol. 16, no. 3, pp. 363-415, 1935.

46. E.J.W. Verwey, "Theory of the stability of lyophobic colloids," *Journal of Physical and Colloid Chemistry*, vol. 51, no. 3, pp. 631-636, 1947.

47. E.J.W. Verwey and J.T.G. Overbeek, "Theory of the stability of lyophobic colloids," *Journal of Colloid Science*, vol. 10, no. 2, pp. 224-225, 1955.

48. E.J.W. Verwey and J.T.G. Overbeek*Theory of the Stability of Lyophobic Colloids*, 1948.

49. S.P.A. Fodor, J.L. Read, M.C. Pirrung, L. Stryer, A.T. Lu, and D. Solas, "Light-directed, spatially addressable parallel chemical synthesis," *Science*, vol. 251, no. 4995, pp. 767-773, 1991.

50. R.G. Nuzzo and D.L. Allara, "Adsorption of bifunctional organic disulfides on gold surfaces," *Journal of the American Chemical Society*, vol. 105, no. 13, pp. 4481-4483, 1983.

51. T. Wink, S.J. Van Zuilen, A. Bult, and W.P. Van Bennekom, "Self-assembled monolayers for biosensors," *Analyst*, vol. 122, no. 4, pp. 43R-50R, 1997.

52. D.M. Collard and M.A. Fox, "Use of electroactive thiols to study the formation and exchange of alkanethiol monolayers on gold," *Langmuir*, vol. 7, no. 6, pp. 1192-1197, 1991.

53. Y.F. Liu, Y.C. Yang, and Y.L. Lee, "Assembly behavior and monolayer characteristics of OH-terminated alkanethiol on Au(111): In situ scanning tunneling microscopy and electrochemical studies," *Nanotechnology*, vol. 19, no. 6, 2008.

54. H. Berney, J. West, E. Haefele, J. Alderman, W. Lane, and J.K. Collins, "DNA diagnostic biosensor: development, characterisation and performance," *Sensors and Actuators, B: Chemical*, vol. 68, no. 1, pp. 100-108, 2000.

55. M.W. Dashiell, A.T. Kalambur, R. Leeson, K.J. Roe, J.F. Rabolt, and J. Kolodzey, "Electrical Effects of DNA as the Gate Electrode of MOS transistors," *Proceedings IEEE Lester Eastman Conference on High Performance Devices*, pp. 259-264, 2002.

56. D.S. Kim, Y.T. Jeong, H.K. Lyu, H.J. Park, H.S. Kim, J.K. Shin, P. Choi, J.H. Lee, G. Lim, and M. Ishida, "Fabrication and characteristics of a field effect transistor-type charge sensor for detecting deoxyribonucleic acid sequence," *Japanese Journal of Applied Physics, Part 1: Regular Papers and Short Notes and Review Papers*, vol. 42, no. 6 B, pp. 4111-4115, 2003.

57. D.S. Kim, Y.T. Jeong, H.J. Park, J.K. Shin, P. Choi, J.H. Lee, and G. Lim, "An FET-type charge sensor for highly sensitive detection of DNA sequence," *Biosensors and Bioelectronics*, vol. 20, no. 1, pp. 69-74, 2004.

58. D.S. Kim, H.J. Park, H.M. Jung, J.K. Shin, P. Choi, J.H. Lee, and G. Lim, "Field effect transistor-based bimolecular sensor employing a Pt reference electrode for the detection of deoxyribonucleic acid sequence," *Japanese Journal of Applied Physics, Part 1: Regular Papers and Short Notes and Review Papers*, vol. 43, no. 6 B, pp. 3855-3859, 2004.

59. G. Libo, H. Jinghong, Z. Hong, and C. Xiang, "DNA field-effect transistor," *Proc. SPIE*, vol. 4414, pp. 47-49, 2001.

60. F.K. Perkins, L.M. Tender, S.J. Fertig, and M.C. Peckerar, "Sensing macromolecules with microelectronics," *Proceedings of SPIE - The International Society for Optical Engineering*, vol. 4608, pp. 251-265, 2002.

61. F. Pouthas, C. Gentil, D. Coì,te, and U. Bockelmann, "DNA detection on transistor arrays following mutation-specific enzymatic amplification," *Applied Physics Letters*, vol. 84, no. 9, pp. 1594-1596, 2004.

62. E. Souteyrand, J.P. Cloarec, J.R. Martin, C. Wilson, I. Lawrence, S. Mikkelsen, and M.F. Lawrence, "Direct detection of the hybridization of synthetic homo-oligomer DNA sequences by field effect," *Journal of Physical Chemistry B*, vol. 101, no. 15, pp. 2980-2985, 1997.

63. F. Uslu, S. Ingebrandt, D. Mayer, S. Boì^cker-Meffert, M. Odenthal, and A. Offenhaì^usser, "Labelfree fully electronic nucleic acid detection system based on a field-effect transistor device," *Biosensors and Bioelectronics*, vol. 19, no. 12, pp. 1723-1731, 2004.

64. F. Wei, B. Sun, Y. Guo, and X.S. Zhao, "Monitoring DNA hybridization on alkyl modified silicon surface through capacitance measurement," *Biosensors and Bioelectronics*, vol. 18, no. 9, pp. 1157-1163, 2003.

65. S.M. Sze*Physics of Semiconductor Devices, 2nd Ed, New York: Wiley, 1981, Pp.*, 2006.

66. H.C. Montgomery, "Field Effect in Germanium at High Frequencies," *Physical Review*, vol. 106, no. 3, pp. 441, 1957.

67. M. Keusgen, M. Ju?nger, I. Krest, and M.J. Scho?ning, "Biosensoric detection of the cysteine sulphoxide alliin," *Sensors and Actuators, B: Chemical*, vol. 95, no. 1-3, pp. 297-302, 2003.

68. A. Poghossian, S. Ingebrandt, M.H. Abouzar, and M.J. Scho?ning, "Label-free detection of charged macromolecules by using a field-effect-based sensor platform: Experiments and possible mechanisms of signal generation," *Applied Physics A: Materials Science and Processing*, vol. 87, no. 3, pp. 517-524, 2007.

69. E.H. Nicollian and J.R. Brews*MOS Physics and Technology Wiley, New York*, 2007.

70. R.G. Sosnowski, E. Tu, W.F. Butler, J.P. O'Connell, and M.J. Heller, "Rapid determination of single base mismatch mutations in DNA hybrids by direct electric field control," *Proceedings of the National Academy of Sciences of the United States of America*, vol. 94, no. 4, pp. 1119-1123, 1997.

71. S.O. Kelley, J.K. Barton, N.M. Jackson, L.D. McPherson, A.B. Potter, E.M. Spain, M.J. Allen, and M.G. Hill, "Orienting DNA helices on gold using applied electric fields," *Langmuir*, vol. 14, no. 24, pp. 6781-6784, 1998.

72. J. Cheng, E.L. Sheldon, A. Uribe, L.O. Gerrue, J. Carrino, M.J. Heller, and J.P. O'Connell, "Preparation and hybridization analysis of DNA/RNA from E. coli on microfabricated bioelectronic chips," *Nat. Biotechnol*, vol. 16, no. 6, pp. 541-546, 1998.

73. C.F. Edman, D.E. Raymond, D.J. Wu, E. Tu, R.G. Sosnowski, W.F. Butler, M. Nerenberg, and M.J. Heller, "Electric field directed nucleic acid hybridization on microchips," *Nucleic Acids Research*, vol. 25, no. 24, pp. 4907-4914, 1997.

74. C. Gurtner, E. Tu, N. Jamshidi, R.W. Haigis, T.J. Onofrey, C.F. Edman, R. Sosnowski, B. Wallace, and M.J. Heller, "Microelectronic array devices and techniques for electric field enhanced DNA hybridization in low-conductance buffers," *Electrophoresis*, vol. 23, no. 10, pp. 1543-1550, 2002.

75. M.J. Heller, A.H. Forster, and E. Tu, "Active microelectronic chip devices which utilize controlled electrophoretic fields for multiplex DNA hybridization and other genomic applications," *Electrophoresis*, vol. 21, no. 1, pp. 157-164, 2000.

76. M. Chee, R. Yang, E. Hubbell, A. Berno, X.C. Huang, D. Stern, J. Winkler, D.J. Lockhart, M.S. Morris, and S.P.A. Fodor, "Accessing genetic information with high-density DNA arrays," *Science*, vol. 274, no. 5287, pp. 610-614, 1996.

77. P.N. Gilles, D.J. Wu, C.B. Foster, P.J. Dillon, and S.J. Chanock, "Single nucleotide polymorphic discrimination by an electronic dot blot assay on semiconductor microchips," *Nature Biotechnology*, vol. 17, no. 4, pp. 365-370, 1999.